Supplementary Information

Bioorthogonal release of sulfonamides and mutually orthogonal liberation of two drugs

Zhuzhou Shao,[1] Wei Liu,[1] Huimin Tao,[1] Fang Liu,[1] Ruxin Zeng,[1] Pier Alexandre Champagne,[2] Yang Cao,[3] K. N. Houk*,[2] and Yong Liang*,[1]

[1]State Key Laboratory of Coordination Chemistry, Jiangsu Key Laboratory of Advanced Organic Materials, School of Chemistry andChemical Engineering, Nanjing University, Nanjing 210023, China

[2]Department of Chemistry and Biochemistry, University of California, Los Angeles,California 90095, United States

[3]Institute of Future Industrial Technologies, Peking University Shenzhen Graduate School, Shenzhen 518055, China

*E-mails: houk@chem.ucla.edu; yongliang@nju.edu.cn

CONTENTS

Section 1: Computational details

The DFT calculations were performed with Gaussian 09.(1) Geometry optimizations of all the minima and transition structures were carried out at the M06-2X level of theory(2) with the 6-31G(d) basis set. Vibrational frequencies were computed at the same level to verify that optimized structures are energy minima or transition states and to evaluate zero-point vibrational energies (ZPVE) and thermal corrections at 298 K. A quasiharmonic correction was applied during the entropy calculation by setting all positive frequencies that are less than 100 cm^{-1} to 100 cm^{-1}.(3) Solvent effects in water were evaluated at the more accurate M06-2X/6-311+G(d,p) level with the CPCM model,(4) using the gas-phase optimized structures. The predicted second-order rate constants shown in Fig. 3 were calculated according to Eyring equation at 298 K, in which the corrected activation free energies [$\Delta G^{\ddagger}$_corr = ($\Delta G^{\ddagger}$_compt + 8.4)/1.6] were used.(5)

References

(1) Frisch, M. J.; Trucks, G. W.; Schlegel, H. B.; Scuseria, G. E.; Robb, M. A.; Cheeseman, J. R.; Scalmani, G.; Barone, V.; Mennucci, B.; Petersson, G. A.; Nakatsuji, H.; Caricato, M.; Li, X.; Hratchian, H. P.; Izmaylov, A. F.; Bloino, J.; Zheng, G.; Sonnenberg, J. L.; Hada, M.; Ehara, M.; Toyota, K.; Fukuda, R.; Hasegawa, J.; Ishida, M.; Nakajima, T.; Honda, Y.; Kitao, O.; Nakai, H.; Vreven, T.; Montgomery, J. A., Jr.; Peralta, J. E.; Ogliaro, F.; Bearpark, M.; Heyd, J. J.; Brothers, E.; Kudin, K. N.; Staroverov, V. N.; Keith, T.; Kobayashi, R.; Normand, J.; Raghavachari, K.; Rendell, A.; Burant, J. C.; Iyengar, S. S.; Tomasi, J.; Cossi, M.; Rega, N.; Millam, J. M.; Klene, M.; Knox, J. E.; Cross, J. B.; Bakken, V.; Adamo, C.; Jaramillo, J.; Gomperts, R.; Stratmann, R. E.; Yazyev, O.; Austin, A. J.; Cammi, R.; Pomelli, C.; Ochterski, J. W.; Martin, R. L.; Morokuma, K.; Zakrzewski, V. G.; Voth, G. A.; Salvador, P.; Dannenberg, J. J.; Dapprich, S.; Daniels, A. D.; Farkas, O.; Foresman, J. B.; Ortiz, J. V.; Cioslowski, J.; Fox, D. J.*Gaussian 09, revision D.01*; Gaussian Inc., Wallingford, CT, 2013.

(2) (a) Zhao, Y.; Truhlar, D. G. *Theor. Chem. Acc.* **2008**, *120*, 215. (b) Zhao, Y.; Truhlar, D. G. *Acc. Chem. Res.***2008**, *41*, 157.

(3) (a) Zhao, Y.; Truhlar, D. G. *Phys. Chem. Chem. Phys.***2008**, *10*, 2813. (b) Ribeiro, R. F.; Marenich, A. V.; Cramer, C. J.; Truhlar, D. G. *J. Phys. Chem. B***2011**, *115*, 14556.

(4) (a) Barone, V.; Cossi, M. *J. Phys. Chem. A* **1998**, *102*, 1995. (b) Cossi, M.; Rega, N.; Scalmani, G.; Barone, V. *J. Comput. Chem.* **2003**, *24*, 669. (c) Takano, Y.; Houk, K. N. *J. Chem. Theory Comput.***2005**, *1*, 70.

(5) Liu, F.; Liang, Y.; Houk, K. N.*Acc. Chem. Res.***2017**, *50*, 2297.

DFT-Computed Energies and Cartesian Coordinates

DIBAC

***G*(water) = -785.235093 Hartree**

C	1.792874	-1.272296	0.126711
C	1.745302	0.101539	-0.228318
C	2.934150	0.759350	-0.538324
C	4.154740	0.094635	-0.457710
C	4.199516	-1.249526	-0.094739
C	3.022046	-1.932408	0.185954
H	2.893238	1.799067	-0.849368
H	5.070937	0.626362	-0.693658
H	5.151013	-1.768365	-0.039702
H	3.040084	-2.982878	0.456690
C	0.511670	-1.854456	0.359067

C	-0.700455	-1.811226	0.393815
C	-1.973158	-1.207373	0.158655
C	-3.202887	-1.651505	0.647399
C	-1.881186	-0.014442	-0.597546
C	-4.349338	-0.905905	0.399387
H	-3.247866	-2.569310	1.224231
C	-3.038413	0.726491	-0.809560
C	-4.265882	0.284912	-0.319439
H	-5.307407	-1.247608	0.778171
H	-2.967716	1.665686	-1.350525
H	-5.159573	0.875285	-0.496177
C	-0.559765	0.402912	-1.220638
N	0.502604	0.794068	-0.268845
H	-0.159080	-0.422280	-1.814735
H	-0.741841	1.253657	-1.883558
C	0.261942	1.962841	0.427708
O	-0.731419	2.626376	0.188166
C	1.239576	2.360256	1.516372
H	1.700126	1.498114	2.002256
H	2.035686	2.988962	1.107396
H	0.681126	2.951026	2.242812

4a

***G*(water) = -1136.102398 Hartree**

C	4.966951	-0.915499	0.180303
C	4.700206	0.390602	0.585567
C	3.413486	0.907382	0.486112
C	2.413706	0.092390	-0.032413
C	2.656096	-1.210471	-0.450041
C	3.947868	-1.712861	-0.334951
H	5.972683	-1.313502	0.266274
H	5.493946	1.010629	0.988350
H	3.177195	1.917165	0.802109
H	1.857471	-1.809766	-0.874812
H	4.156499	-2.727388	-0.657044
C	-0.064329	-0.073043	0.006910
H	-0.124327	-1.105221	0.301178
N	1.080314	0.615809	-0.143538
N	0.932070	1.872949	-0.416878
O	-0.405758	2.053190	-0.444278
C	-1.083183	0.884410	-0.196465
N	-2.377735	0.935377	-0.190593
S	-3.158809	-0.499601	0.021450
O	-3.661405	-0.989638	-1.254881
O	-2.361075	-1.417812	0.843472
C	-4.546129	0.046852	0.990897
H	-4.178613	0.438005	1.939435
H	-5.075895	0.815346	0.428175
H	-5.182705	-0.825093	1.150171

TS_4a-DIBAC

***G*(water) = -1921.303201 Hartree**

C	-0.327787	-1.513386	0.689240
C	0.696322	-2.491006	0.750266
C	0.461761	-3.699889	1.405089
C	-0.750457	-3.945518	2.040787
C	-1.755365	-2.983797	1.999710
C	-1.545681	-1.785260	1.326506
H	1.244137	-4.453345	1.400050
H	-0.911042	-4.890226	2.550366
H	-2.710131	-3.162476	2.484122
H	-2.346244	-1.053874	1.285553
C	-0.063526	-0.291768	-0.034122
C	0.743104	0.362257	-0.739608
C	1.987192	0.443606	-1.469106
C	2.560784	1.652582	-1.880196
C	2.652494	-0.771615	-1.735638
C	3.783575	1.657055	-2.539169
H	2.039631	2.580683	-1.679360
C	3.880957	-0.745917	-2.386951
C	4.446357	0.458879	-2.793081
H	4.221301	2.599621	-2.853056
H	4.402374	-1.683833	-2.552567
H	5.405988	0.462551	-3.300553
C	2.025193	-2.082457	-1.328140
N	1.950127	-2.257113	0.133513
H	1.002111	-2.145424	-1.707910
H	2.606701	-2.910228	-1.745111
C	3.160564	-2.417574	0.780557
O	4.197017	-2.479700	0.144242
C	3.157118	-2.454754	2.296767
H	2.321339	-1.902715	2.730303
H	3.111663	-3.486928	2.655321
H	4.104839	-2.026823	2.625299
C	1.452057	4.055737	3.069509
C	1.311048	4.674585	1.828487

C	0.546007	4.079282	0.833079
C	-0.063191	2.855882	1.098324
C	0.079790	2.213716	2.324656
C	0.837222	2.830692	3.315124
H	2.044534	4.528709	3.845909
H	1.789758	5.629276	1.637699
H	0.406384	4.546780	-0.135914
H	-0.371934	1.240355	2.488732
H	0.957169	2.343754	4.277175
C	-1.752659	1.275575	0.226931
H	-2.362410	1.189350	1.111620
N	-0.834169	2.247122	0.068077
N	-0.258376	2.143706	-1.128136
O	-1.235603	1.560262	-1.913302
C	-2.158667	0.951954	-1.125736
N	-3.093503	0.288447	-1.706922
S	-4.386804	-0.244880	-0.824912
O	-4.175405	-0.061721	0.618191
O	-5.600187	0.291659	-1.413750
C	-4.311744	-1.989835	-1.167100
H	-4.357984	-2.127754	-2.247340
H	-3.382118	-2.388359	-0.756472
H	-5.177133	-2.444317	-0.681155

ABNBD

***G*(water) = -632.8655149 Hartree**

C	-4.611234	0.207384	-1.142146
C	-3.238328	0.178259	-1.446721
C	-2.369606	0.780346	-0.565174
C	-2.837622	1.407068	0.600824
C	-4.180057	1.442613	0.905393
C	-5.073131	0.826995	0.009942
H	-5.318151	-0.26741	-1.815678
H	-2.881645	-0.317458	-2.345459
H	-4.546903	1.922313	1.808857
H	-6.136645	0.832257	0.228128
C	-1.021406	3.048081	0.402848
C	-0.588206	2.451211	-0.702581
H	-1.071307	4.103957	0.634701
H	-0.186074	2.895933	-1.605115
C	-0.833999	0.939807	-0.545801
C	-1.572095	1.934907	1.298381
H	-1.641282	2.144153	2.364763
C	-0.016394	0.039252	-1.443271
H	1.0478450	0.157311	-1.223175
H	-0.284941	-1.006894	-1.30571
H	-0.188744	0.330862	-2.485239
N	-0.620213	0.853060	0.934006
C	-0.620942	-0.363624	1.592681
O	-0.333145	-1.408452	1.042588
C	-0.948699	-0.298670	3.071627
H	-0.669787	-1.250746	3.521764
H	-0.420296	0.519059	3.568835
H	-2.025917	-0.144382	3.203812

TS_4a-ABNBD

***G*(water) = -1768.924555 Hartree**

C	8.734341	-2.799660	3.413217
C	8.541204	-1.452772	3.124386
C	7.269044	-0.961709	2.851639
C	6.191898	-1.843709	2.846159
C	6.364688	-3.190266	3.157437
C	7.641021	-3.661863	3.438239
H	9.730185	-3.176966	3.619288
H	9.385437	-0.771606	3.111529
H	7.103959	0.088861	2.643312
H	5.520898	-3.872109	3.163734
H	7.778436	-4.713292	3.670362
C	3.715606	-2.015345	2.521006
H	3.558915	-2.984270	2.967708
N	4.892134	-1.348601	2.546299
N	4.756565	-0.160041	1.960791
O	3.415537	0.158604	2.194180
C	2.725962	-0.966859	2.476623
N	1.443025	-0.898061	2.590367
S	0.670504	-2.343226	2.824951
O	0.327380	-2.913516	1.524209
O	1.392685	-3.195014	3.774123
C	-0.816865	-1.767476	3.606372
H	-0.550599	-1.293371	4.551048
H	-1.304525	-1.060826	2.935119
H	-1.444791	-2.643931	3.774102
C	4.729860	-2.170470	-4.386792
C	5.286227	-1.407530	-3.345932
C	5.099787	-1.847173	-2.053721
C	4.370513	-3.014736	-1.783023

C	3.814999	-3.764561	-2.796909
C	4.008742	-3.326195	-4.117961
H	4.870466	-1.853384	-5.415581
H	5.854585	-0.507180	-3.562906
H	3.246836	-4.667110	-2.590120
H	3.589935	-3.900696	-4.938438
C	3.510936	-1.987887	0.259859
C	4.246439	-0.835505	-0.016179
H	2.428275	-2.062112	0.238769
H	3.817601	0.132355	-0.244941
C	5.549674	-1.289702	-0.685744
C	4.382471	-3.140738	-0.253390
H	4.190159	-4.127094	0.166372
C	6.690398	-0.299606	-0.698552
H	7.033990	-0.095239	0.316495
H	7.532470	-0.673567	-1.280217
H	6.327177	0.636250	-1.137527
N	5.714707	-2.580169	0.046737
C	6.886891	-3.310352	0.032949
O	7.977141	-2.783862	-0.078489
C	6.735488	-4.808944	0.206032
H	7.725121	-5.225903	0.391383
H	6.067743	-5.065609	1.032411
H	6.323426	-5.243381	-0.712331

Section 2: Materials and instrumentation

Chemical reagents were obtained from commercial sources (Energy Chemical, Innochem, J&K Scientific) and used without further purification. All reactions were monitored by TLC with silica gel-coated plates with 0.2 mm silica gel-coated HSGF 254 plates. Compounds were purified by column chromatography on silica gel (200-300 mesh) or neutrality Al_2O_3 (200-300 mesh) eluting with a gradient (petroleum ether / ethyl acetate).

Nuclear magnetic resonance spectrawere recorded on a Bruker Ascend^{TM} 400 or 500 or 600 spectrometer at 295.15 K. Chemical shifts for ^{1}H NMR spectra are reported as δ in units of parts per million (ppm) downfield from $SiMe_4$ (δ 0.0) and relative to the signal of chloroform-d (δ 7.26, singlet) or dimethyl sulfoxide-d_6 (δ 2.50, quintet). Multiplicities were given as: s (singlet); d (doublet); t (triplet); q (quartet); dd (doublets of doublet) or m (multiplets). The number of protons (n) for a given resonance is indicated by nH. Coupling constants are reported as a J value in Hz. Chemical shifts for ^{13}C NMR spectra are reported as δ in units of parts per million (ppm) downfield from $SiMe_4$ (δ 0.0) and relative to the signal of chloroform-d (δ 77.16, triplet) or dimethyl sulfoxide-d_6 (δ 39.52, heptet). ^{19}F NMR spectra were recorded on Bruker Ascend^{TM} 500 (470 MHz) and were referenced relative to CF_3COOH(neat) at δ -78.5 ppm. Mass spectra were obtained using BOHUI-Advion expression ^{s}TLC-CMS. High-resolution mass spectra (HRMS) analyses were performed on a Thermo Scientific ltq-orbitrap XL mass spectrometer. Melting points of solids were obtained using a GLO X-5 series micro melting point apparatus and were uncorrected.

Liquid chromatogram was detected by Shimadzu UFLC (LC-20AD,SPD-M20Adetector). Analyses were performed using an ACE Excel 5 AQ column (4.6 x 250 mm, 5 μm), a flow rate of 1.0 mL min^{-1} and typically a ratio ranger from 80% to 70% acetonitrile in water.

A vertical heating pressure steam sterilizer CDZM-60KCS-III was used for the sterilization of vessels. The operations were done on the Aietech SW-CJ-1FD type clean bench. Fetal bovine serum was collected in Canada and processed in the US (HyClone). The PBS and serum were cultivated in an electro-heating standing-temperature cultivator (MD:HPX-9052 MBE) at 37 °C. The COX-2 activities were observed with a Tecan Sunrise (Auatria GmbH) at 415 nm. Human COX-2 ELISA Kits (catalog No.460121), PGE2 enzyme immunoassay (EIA) kit-monoclonal (catalog No.414026) and Heme (catalog No. 460102) were purchased from Cayman Chemical.

Section 3: Organic synthesis

Synthesis of celecoxib (CXB) 8c

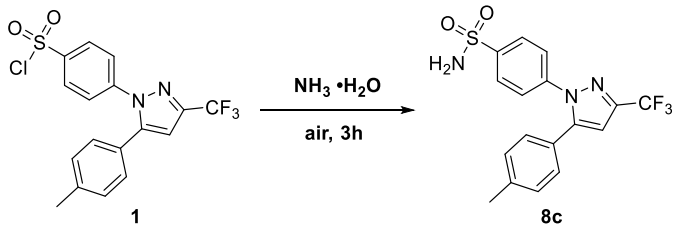

4-(5-(p-tolyl)-3-(trifluoromethyl)-1H-pyrazol-1-yl)benzenesulfonyl chloride **1** was prepared according to a literature protocol.[1]

To a 25 mL round-bottom flask with 5 mL ammonium hydroxide solution (28%) added **1** (290 mg, 1.47 mmol) at 0℃, and stirred 3 h in air. The mixture was diluted with 5 mL water, and extracted with Et_2O (3x15 mL). The separated organic layer was again washed with brine (2×50 mL) and concentrated *in vacuo*. The crude was recrystallized from ice-cold ethanol to give the product **8c** as white solid in a yield of 500 mg (89%).

M.p.: 162-163°C. **^{1}H NMR** (500 MHz, $CDCl_3$) δ 7.90 (d, *J* = 8.7 Hz, 2H), 7.47 (d, *J* = 8.7 Hz, 2H), 7.18 (d, *J* = 8.0 Hz, 2H), 7.11 (d, *J* = 8.1 Hz, 2H), 6.74 (s, 1H), 5.05 (s, 2H), 2.38 (s, 3H). **^{13}C NMR** (125 MHz, $CDCl_3$) δ 145.2, 144.1 (q, J_{C-F}=38.7 Hz), 142.5, 141.2, 139.8, 129.8,

[1]Szabó, G.; Fischer, J.; Kis-Varga, A.; Gyires, K. *J. Med. Chem*. **2008**, *51*, 142.

128.7, 127.5, 125.6, 125.5, 121.0 (q, J_{C-F}=269.2 Hz), 106.3 (d, J_{C-F}=1.7 Hz), 21.3. **^{19}F NMR** (470M, $CDCl_3$) -62.43 (s, 3F). The physical data were identical to those previously reported.[2]

Synthesis of sydnonimine hydrochloride 9 and 9'

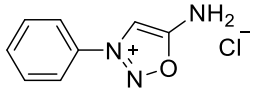

9

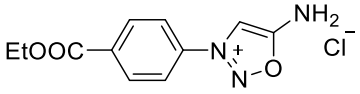

9'

Sydnonimine hydrochloride **9** and **9'** were prepared according to a literature protocol.[3]

9: White solide. **^{1}H NMR** (400 MHz, DMSO-d_6) δ 10.17 (s, 2H), 8.69 (s, 1H), 8.10 – 8.02 (m, 2H), 7.85 – 7.79 (m, 1H), 7.79 – 7.71 (m, 2H). **^{13}C NMR** (100 MHz, DMSO-d_6) δ 169.4, 133.5, 132.8, 130.4, 122.7, 102.2. **HRMS (ESI+):** calcd. for $C_8H_8N_3O^+$ [M-Cl^-]$^+$: 162.0662, found: 162.0659.

9': White solid. **^{1}H NMR** (500 MHz, DMSO-d_6) δ 9.93 (s, 2H), 8.75 (s, 1H), 8.29 (d, *J* = 8.7 Hz, 2H), 8.20 (d, *J* = 8.7 Hz, 2H), 4.39 (q, *J* = 7.1 Hz, 2H), 1.36 (t, *J* = 7.1 Hz, 3H). **^{13}C NMR** (125 MHz, DMSO-d_6) δ 169.6, 164.3, 135.8, 134.1, 131.0, 123.3, 102.8, 61.7, 14.1. **HRMS (ESI+):** calcd. for $C_{11}H_{12}N_3O_3^+$[M-Cl^-]$^+$: 234.0873, found: 234.0873.

General procedure for synthesis of N_6-sulfonyl sydnonimine 4

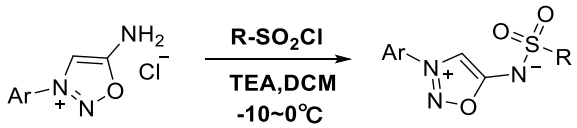

SIN

Ar: Ph 9

4-COOEt-Ph 9'

N_6-sulfonly-SIN

To a solution of **9** or **9'** (2.5 mmol) and sulfonyl chloride (5 mmol) in anhydrous DCM (15 mL) was slowly dropwise added TEA (7.5 mmol, 594 mg) of DCM (5 mL) solution at -10℃, and keep stirred for two hours. Then gradually raised the temperature to 0℃, and stirred constantly for 2 h. The mixture was quenched with water (10 mL). The two layers were separated. The separated organic layer was again washed with brine (2×10mL), dried over $MgSO_4$ and concentrated *in vacuo*. The crude product was purified by column chromatography (Al_2O_3, 200-300 mesh, petroleum ether: ethyl acetate = 5:1 to 2:1, v/v) to give N_6-sulfonyl-SIN **4**.

[2]Ji, G.; Wang, X.; Zhang, S.; Xu, Y.; Ye, Y.; Li, M.; Zhang, Y.; Wang, J. *Chem. Commun.* **2014**, *50*, 4361.
[3]Beal, E. N.; Tumbull, K. *Synth. Commun.* **1992**, *22*, 673.

***(methylsulfonyl)(3-phenyl-1,2,3-oxadiazol-3-ium-5-yl)amide (N_6-Ms-SIN)* 4a**

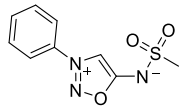

Yellow solid, 472 mg, yield 79%. **M. p.**: 191-192℃. **^{1}H NMR** (400 MHz, DMSO-d_6) δ 8.34 (s, 1H), 8.08–8.03 (m, 2H), 7.81–7.68 (m, 3H), 2.99 (s, 3H).**^{13}C NMR** (100 MHz, DMSO-d_6) δ 170.1, 133.5, 133.1, 130.2, 122.5, 102.2, 41.2.**HRMS (ESI+):** calcd. for $C_9H_{10}N_3O_3S^+$ $[M+H]^+$: 240.0437, found: 240.0436.

***((3-chloropropyl)sulfonyl)(3-(4-(ethoxycarbonyl)phenyl)-1,2,3-oxadiazol-3-ium-5-yl)amide* 4a'**

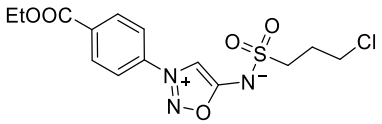

White solid, 841 mg, yield 90%. **^{1}H NMR** (500 MHz, $CDCl_3$) δ 8.34 (d, *J* = 8.5 Hz, 2H), 7.91 (d, *J* = 8.6 Hz, 2H), 7.87 (s, 1H), 4.46 (q, *J* = 7.1 Hz, 2H), 3.73 (t, *J* = 6.3 Hz, 2H), 3.30 (t, *J* = 7.2 Hz, 2H), 2.43–2.32 (m, 2H), 1.45 (t, *J* = 7.1 Hz, 3H). **^{13}C NMR** (125 MHz, $CDCl_3$) δ 170.5, 164.4, 136.4, 135.3, 132.0, 121.8, 100.8, 62.3, 51.7, 43.2, 27.3, 14.4. **HRMS (ESI+):** calcd. for $C_{14}H_{17}ClN_3O_5S^+[M+H]^+$: 374.0572, found: 374.0567.

***(3-phenyl-1,2,3-oxadiazol-3-ium-5-yl)(tosyl)amide (N_6-Ts-SIN)* 4b**

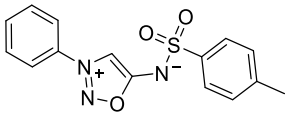

White solid, 615 mg, yield 78%. **M. p.**: 192-193℃. **^{1}H NMR** (400 MHz, DMSO-d_6) δ 8.48 (s, 1H), 8.04 (d, *J* = 7.9 Hz, 2H), 7.82 (d, *J* = 8.2 Hz, 2H), 7.79–7.75 (m, 1H), 7.75–7.68 (m, 2H), 7.33 (d, *J* = 8.0 Hz, 2H), 2.35 (s, 3H). **^{13}C NMR** (100 MHz, DMSO-d_6) δ 169.8, 142.1, 140.0, 133.4, 133.1, 130.2, 129.3, 126.1, 122.6, 102.6, 20.9. **HRMS (ESI+):** calcd. for $C_{15}H_{14}N_3O_3S^+[M+H]^+$: 316.0750, found: 316.0748.

***(3-phenyl-1,2,3-oxadiazol-3-ium-5-yl)((4-(5-(p-tolyl)-3-(trifluoromethyl)-1H-pyrazol-1-yl)phenyl)sulfonyl)amide (N_6-CXB-SIN)* 4c**

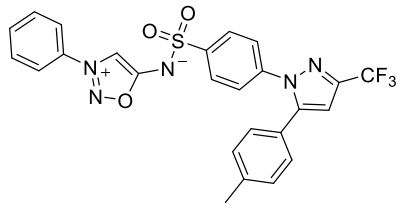

Yellow solid, 998 mg, yield 76%. **M. p.**: 243-244℃. **^{1}H NMR** (600 MHz, DMSO-d_6) δ 8.53 (s, 1H), 8.04 (d, *J* = 7.8 Hz, 2H), 7.99 (d, *J* = 8.6 Hz, 2H), 7.81-7.72 (m, 1H), 7.75-7.70 (m, 2H), 7.49 (d, *J* = 8.6 Hz, 2H), 7.23-7.15 (m, 5H), 2.28 (s, 3H). **^{13}C NMR** (150 MHz, DMSO-d_6) δ 169.9, 145.2, 142.6, 142.2 (q, $J_{C\text{-}F}$=37.5 Hz), 141.3, 139.1, 133.4, 133.2, 130.2, 129.421, 128.8, 127.2, 125.9, 125.3, 122.7, 121.3 (q, $J_{C\text{-}F}$=267 Hz), 106.1, 103.0, 20.8. **^{19}F NMR** (470M, DMSO-d_6) -61.16 (s, 3F). **HRMS** (ESI+)**:** calcd. for $C_{25}H_{19}F_3N_5O_3S^+[M+H]^+$: 526.1155, found: 526.1150.

Synthesis of doxorubicin-prodrug 11 (ABNBD-Dox)

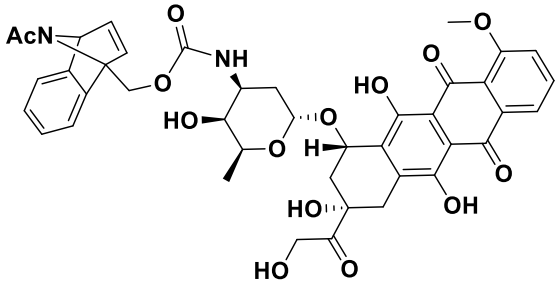

Doxorubicin-prodrug **11** was prepared according to a literature protocol.[4]

Red solid, 25 mg. **^{1}H NMR** (400 MHz, $CDCl_3$) δ 13.92 (s, 1H), 13.17 (s, 1H), 7.98 (d, *J* = 7.6 Hz, 1H), 7.75 (t, *J* = 8.0 Hz, 1H), 7.36 (d, *J* = 8.4 Hz, 1H), 7.23 (s, 2H), 7.05-6.70 (m, 4H), 5.60 – 5.32 (m, 3H), 5.27-5.10 (m, 2H), 4.78 (s, 2H), 4.64 (s, 1H), 4.18-4.09 (m,1H), 4.05 (s, 3H), 3.87 (s, 1H), 3.78 (s, 1H), 3.23 (d, *J* = 18.7 Hz, 1H), 3.10 (s, 2H), 2.95 (d, *J* = 18.8 Hz, 1H), 2.35 (d, *J* = 14.4 Hz, 1H), 2.15 (d, *J* = 12.4 Hz, 1H), 1.93 (s, 3H), 1.88-1.78 (m, 2H), 1.30 (d, *J* = 6.1 Hz, 3H), 1.26 (s, 1H). **MS** (ESI+): 807.4 [M+Na]$^+$.

Section 4: Release studies

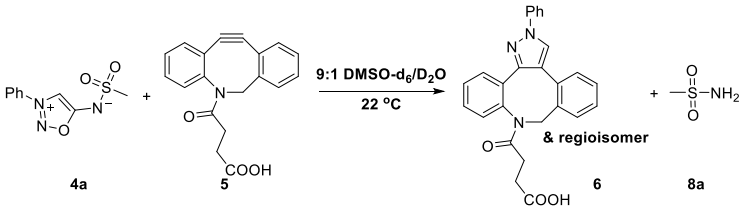

Stock solutions of DIBAC-COOH **5** (10.6 mM) and N_6-Ms-SIN **4a** (15.6 mM) in DMSO-d_6 were prepared. Aliquots of **5** stock solution (124 μL), **4a** solution (76.5 μL), DMSO-d_6 (339.5μL) and D_2O (60 μL) were combined to give final concentrations of 2 mM

[4]Xu, M.; Tu, J.; Franzini, R. M. *Chem. Commun.* **2017**, *53*, 6271.

for **5** and 2.2 mM for **4a**. The sample was incubated at 22 °C and monitored by ^{1}H NMR spectroscopyat several time points (**Figure S1**).

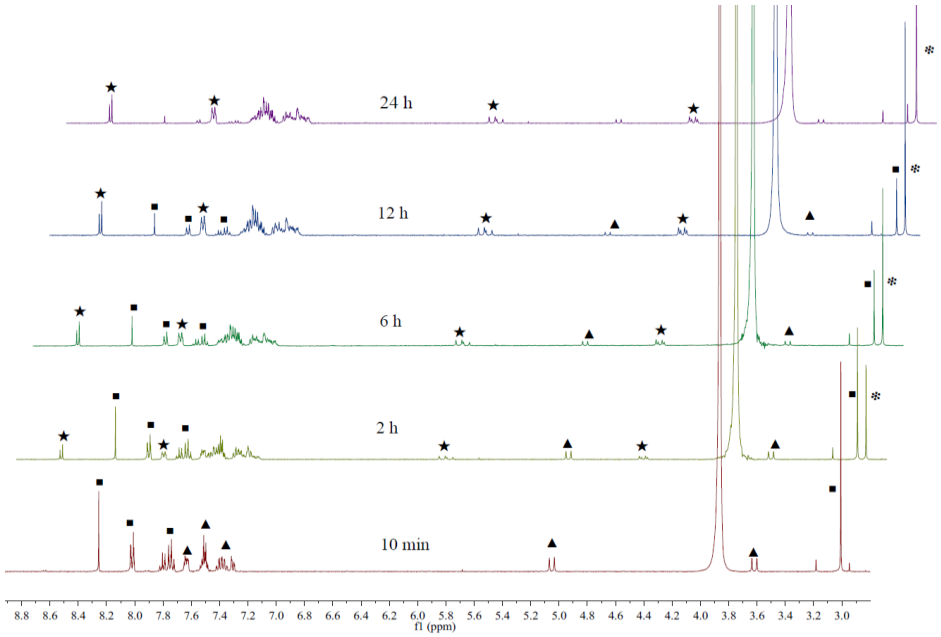

Figure S1. ^{1}H NMR analysis of the reation of N_6-Ms-SIN (2 mM) and DIBAC-COOH (2.2 mM) in DMSO-d_6/D_2O (9:1 v/v). Legend: ■: N_6-Ms-SIN **4a**; ▲: DIBAC-COOH **5**; ★: cycloaddition product **6**; *: $MsNH_2$ **8a**.

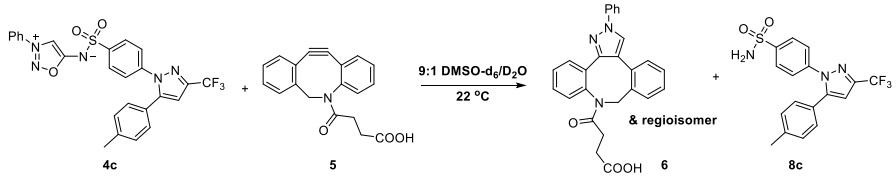

Stock solutions of DIBAC-COOH **5** (10.6 mM) and N_6-CXB-SIN **4c** (15.6 mM) in DMSO-d_6 were prepared. Aliquots of **5** stock solution (226 µL), **4c** solution (76.9 µL), DMSO-d_6 (237.1 µL) and D_2O (60 µL) were combined to give final concentrations of 4 mM for **5** and 2 mM for **4c**. The sample was incubated at 22 °C and monitored by ^{1}H NMR spectroscopy at several time points. The reagent **4c** disappeared and converted into cycloaddition products **6** and **8c** after 22 h (**Figure S2**). Further analysis by TLC-MS was used to determine the release of CXB **8c**: m/z=380.0 $[M-H]^-$ (**Figure S3**).

High-Resolution Mass Spectroscopy of cycloaddition adducts **6**:

HRMS (ESI+): calcd. for $C_{26}H_{22}N_3O_3^+$ $[M+H]^+$: 424.1656, found: 424.1655.

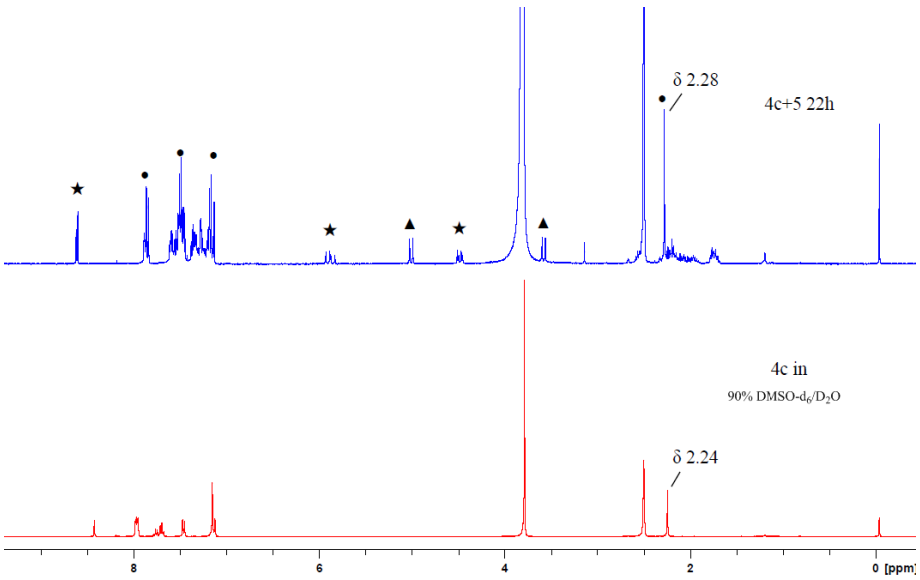

Figure S2. ^{1}H NMR analysis of the reation of N_6-CXB-SIN **4c** (2 mM) and DIBAC-COOH **5** (4 mM) in DMSO-d$_6$/ D$_2$O (9:1 v/v). Legend: ▲: **5**; ★: **6**; ●: **8c**.

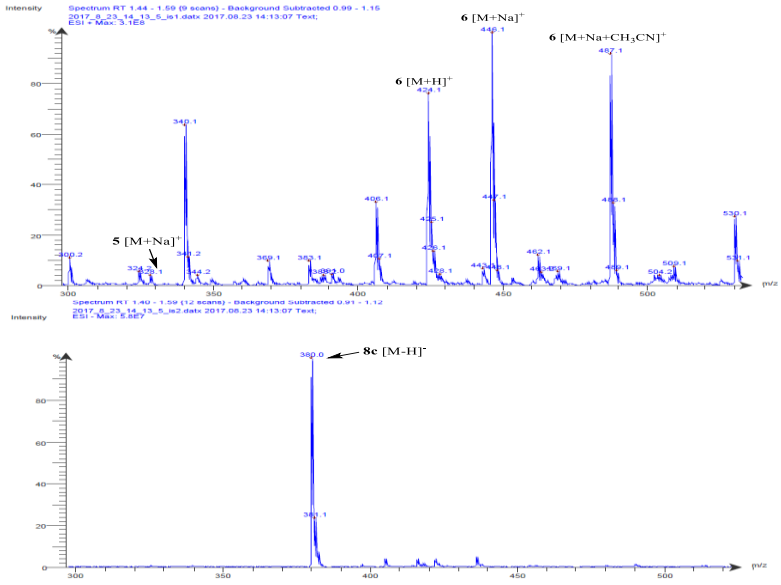

Figure S3. TLC-MS analysis of the reaction of **4c** with **5** in DMSO-d$_6$/D$_2$O (9:1 v/v) after 22 h. The upper graph is MS-spectra in positive mode, the lower graph is MS-spectra in negative mode.

Section 5: Analysis of reaction kinetics

The second-order reaction rate constant of the reaction between DIBAC-COOH **5** and N_6-sulfonyl-SIN **4** was determined under pseudo-first-order conditions in DMSO-d$_6$ /D$_2$O at several time points at 295.15 K. According to the internal standard to calculate the concentration [A] of **4**. Fitted curve –ln[A]~*t*, and performed linear regression analysis (**Equation S1**).

$$-\ln[A] = k_2[B]_0 t + const$$

Equation S1. [A]—concentration of N_6-sulfonyl-SIN **4** (M); $[B]_0$—initial concentration of DIBAC **5**, consider as constant; k_2—second-order rate constant (M^{-1} s^{-1}).

The reaction of **4a** and **4b** with **5** was determind by ^{1}H NMR spectroscopy using 1,3,5-trimethoxybenzene as internal standard. We measured the reaction rate of **4c** and **4a'** with **5** by HPLC using 2,5-dibromopyridine as internal standard. Stock solutions of DIBAC-COOH **5** and N_6-sulfonly-SIN **4** and internal standard (1,3,5-trimethoxybenzene or 2,5-dibromopyridine) in DMSO-d_6 were prepared. Prepared respective concentration solutions of **4** and excess DIBAC-COOH **5** (~10 folds) in 90 % and 50 % DMSO-d_6 /D_2O. The progress of the reaction was monitored by ^{1}H NMR spectroscopy or HPLC at several time points **(Figures S4a-S4g**).

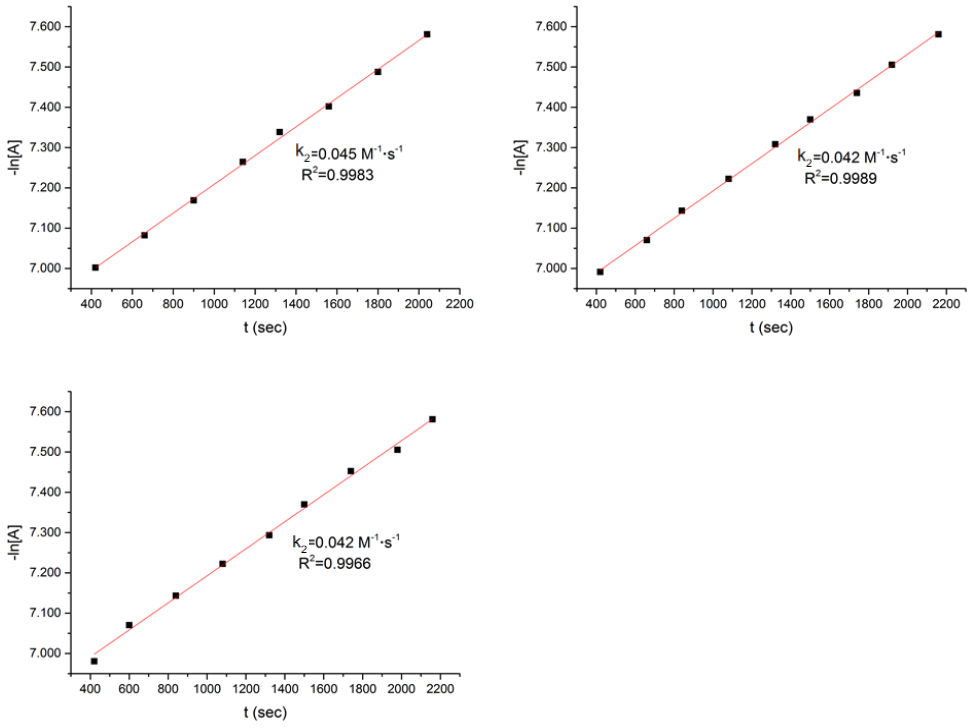

Figure S4a. Kinetic plot of reaction of **4a** with **5** in 90% DMSO-d_6/D_2O; k_2= (0.043±0.004) M^{-1}·s^{-1}, $[B]_0$ = 10 mM.

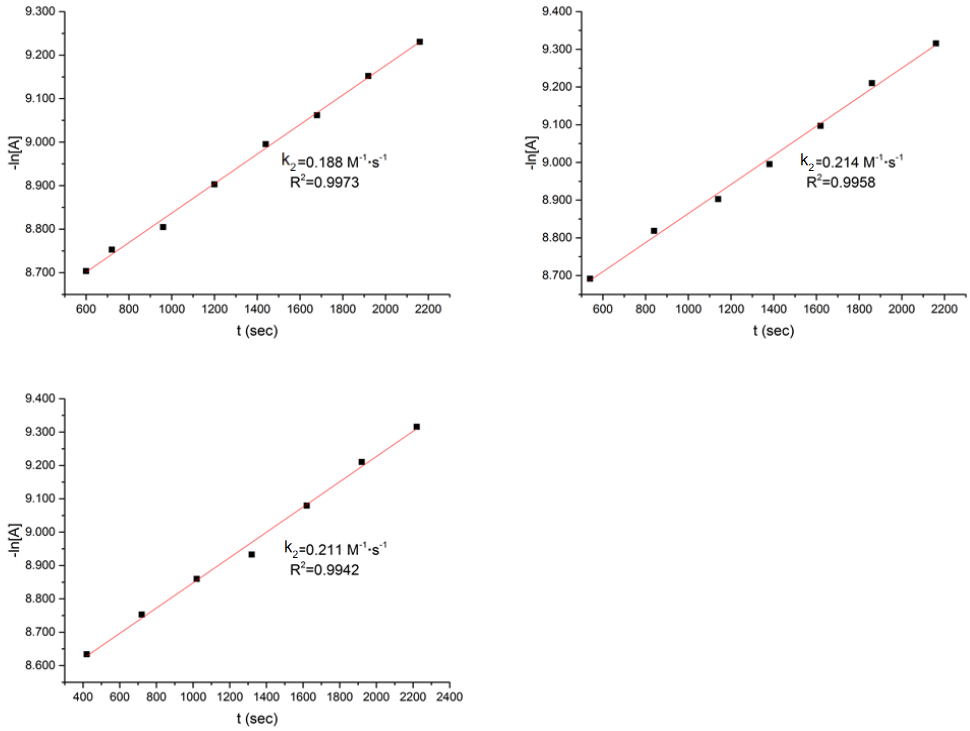

Figure S4b. Kinetic plot of reaction of **4a** with **5** in 50% DMSO-d_6/D_2O; k_2= (0.20±0.03) $M^{-1}\cdot s^{-1}$, $[B]_0$ = 3.0 mM.

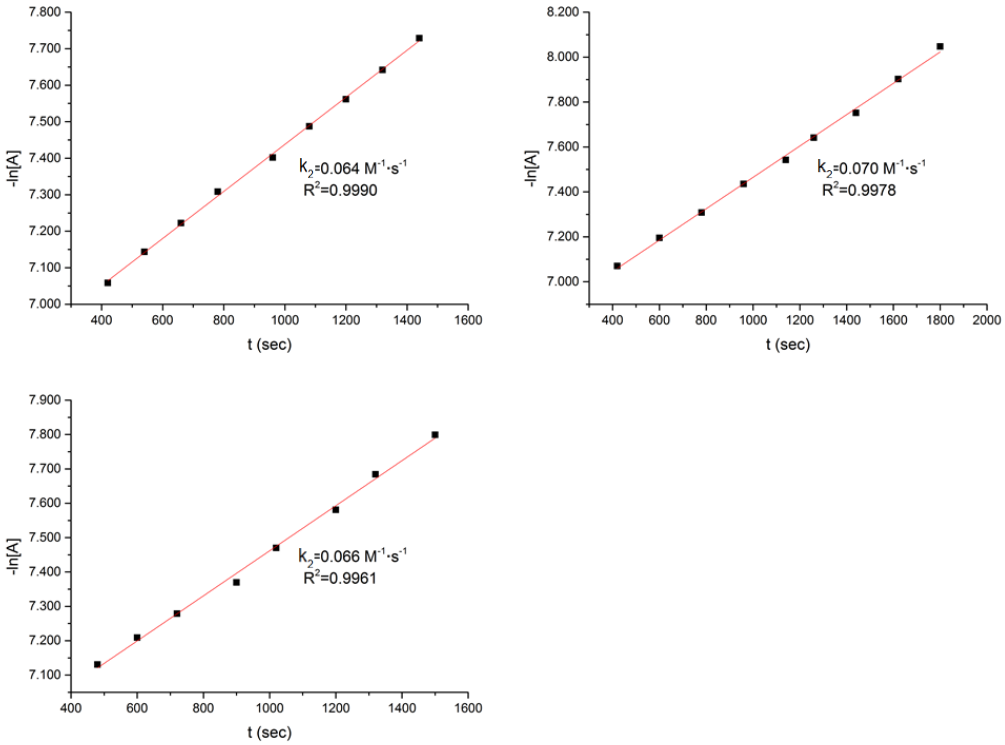

Figure S4c. Kinetic plot of reaction of **4b** with **5** in 90% DMSO-d_6/D_2O; k_2= (0.067±0.008) $M^{-1}\cdot s^{-1}$, $[B]_0$ = 10 mM.

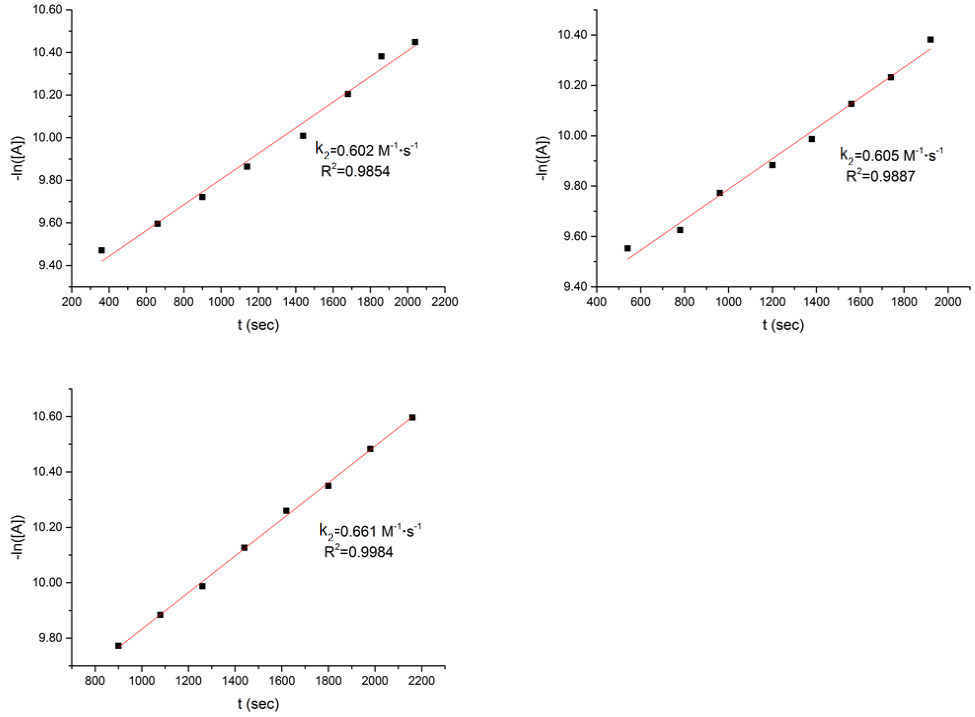

Figure S4d. Kinetic plot of reaction of **4b** with **5** in 50% DMSO-d_6/D_2O; k_2= (0.62±0.08) $M^{-1}\cdot s^{-1}$, $[B]_0$ = 1 mM.

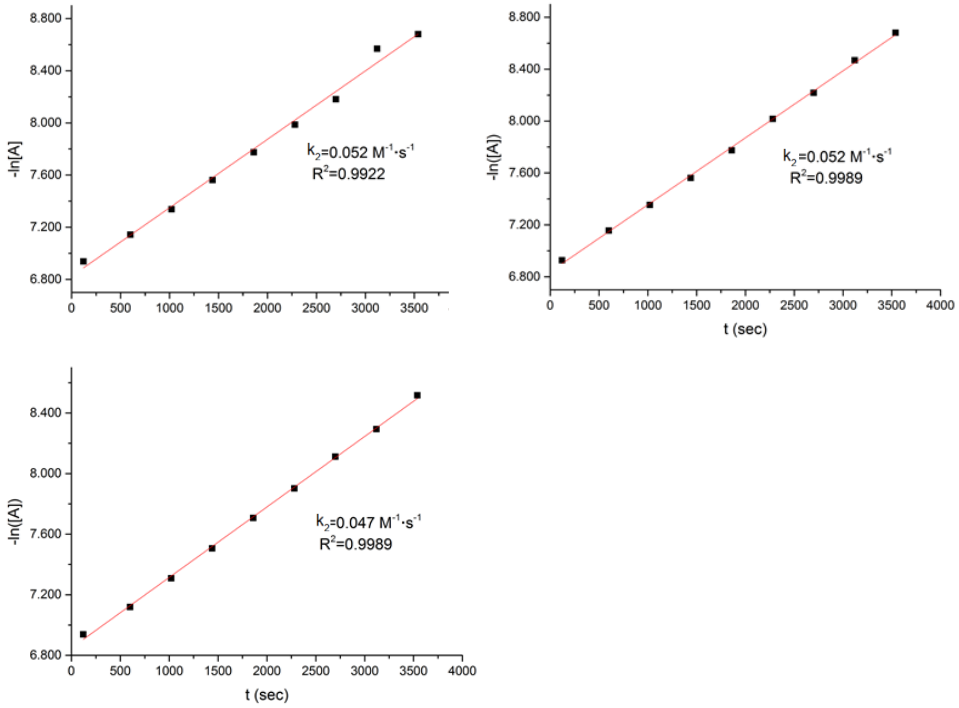

Figure S4e. Kinetic plot of reaction of **4c** with **5** in 90% DMSO-d_6/D_2O; k_2= (0.050±0.007) $M^{-1}\cdot s^{-1}$, $[B]_0$ = 10 mM.

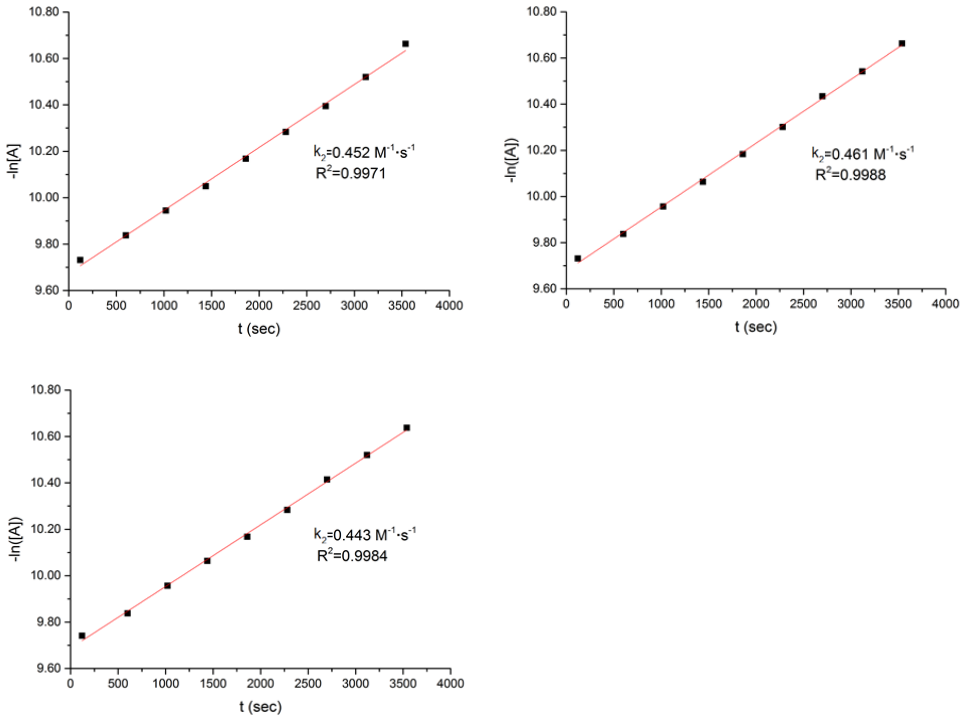

Figure S4f. Kinetic plot of reaction of **4c** with **5** in 50% DMSO/H_2O; k_2= (0.45±0.02) $M^{-1}\cdot s^{-1}$, $[B]_0$ = 0.6 mM.

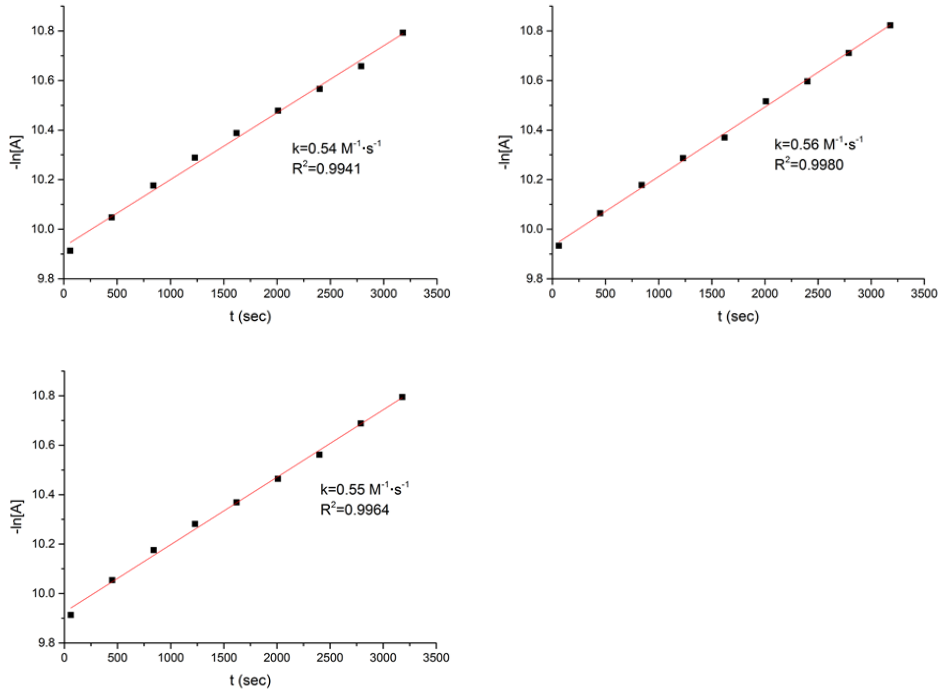

Figure S4g. Kinetic plot of reaction of **4a'** with **5** in 50% DMSO/H_2O; k_2= (0.55±0.02) $M^{-1}\cdot s^{-1}$, $[B]_0$ = 0.5 mM.

Section 6: Stability studies of N_6-CXB-SIN 4c

Stability of 4c in PBS

Stock solutions of N_6-CXB-SIN **4c** (15.6 mM) in DMSO were prepared. Aliquots stock aforementioned solution (20μL), DMSO (2.48 mL) and 0.01 M PBS (2.5 mL) were combined to give final concentration of 62.4 μM for N_6-CXB-SIN in DMSO-PBS (1:1, v/v). The sample was incubated at 37 ºC and analyzed by HPLC at 280 nm at a series of time points. No free drug CXB or other side products were observed (**Figure S5**).

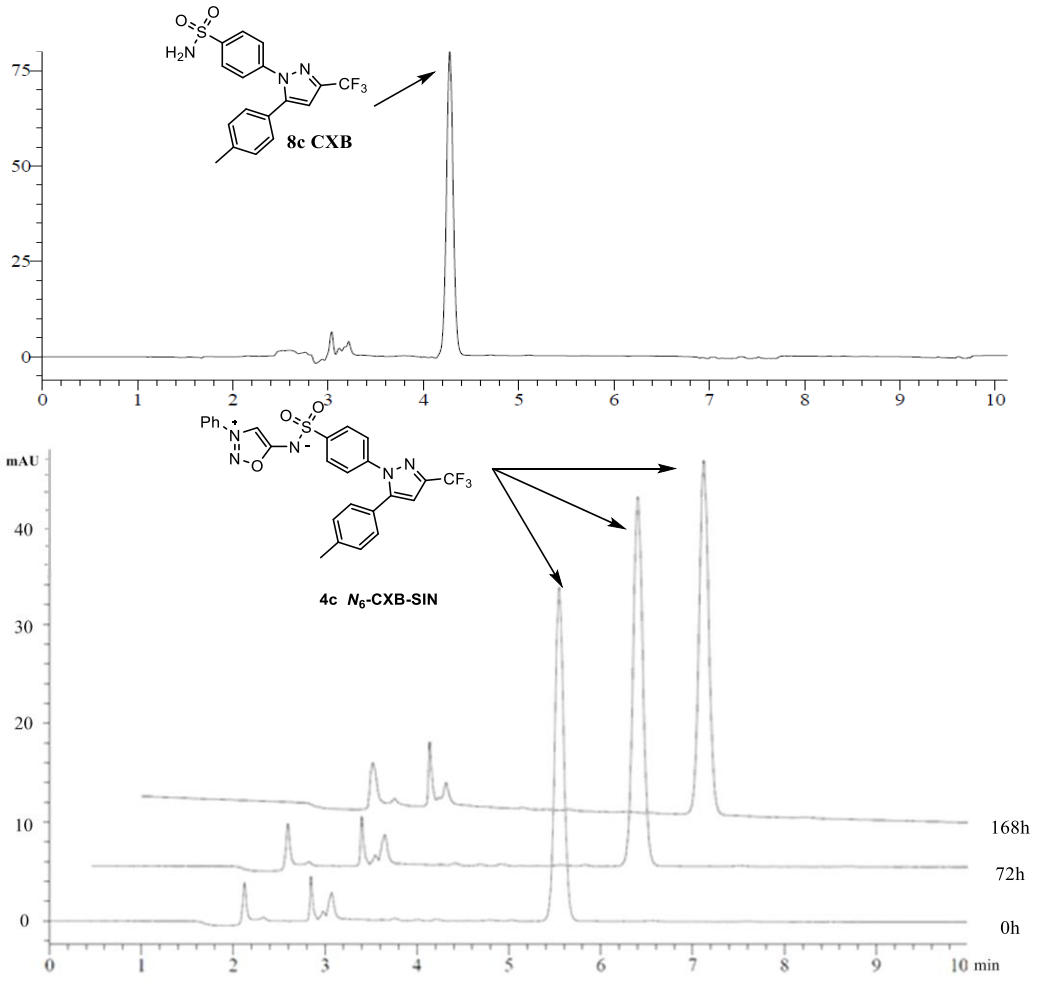

Figure S5. HPLC determined of N_6-CXB-SIN **4c** in DMSO-PBS (1:1, v/v) in different time points (lower graph), and the retention time of **8c CXB** (upper graph). The mobile phase ratio was 80% CH_3CN/H_2O, flow rate of 1.0 mL/min. Retention time for **4c**: 5.53 min; CXB for 4.20 min.

Stability of 4c in FBS:PBS (1:1 v/v)

Stock solutions of N_6-CXB-SIN **4c** (15.6 mM) in DMSO were prepared. Aliquots of **4c** stock solution (57.7 μL), 0.01 M PBS (2.5 mL) and fetal bovline serum (2.5mL) (HyClone, USA) were combined to give PBS/Serum (1:1, v/v) solution. The sample was thoroughly mixed and incubated at 37℃ in the dark, and subsequently a 250 μL aliquot of the sample was taken at indicated time points and quenched by 0.5 mL ice-cold acetonitrile, followed by centrifugation at 13000 rpm for 10 min. The supernatant was injected and analysis by HPLC at 260 nm. The rate of decay of **4c** is calculated through these data (**Figure S6**).

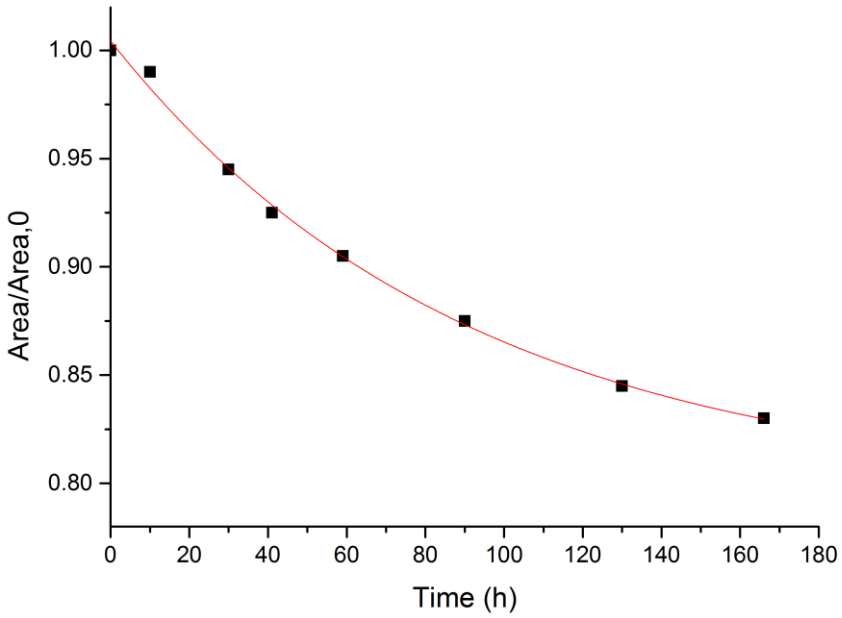

Figure S6. Decrease of absorption at 260 nm of a solution of N_6-CXB-SIN **4c** in FBS/PBS (1:1 v/v). The results are expressed as the mean (n=3).

Section 7: Cyclooxygenase-2 inhibition assay

The COX-2 inhibition (IC_{50} values, μM) was determined using a human COX-2 ELISA Kit (catalog number 460121, Cayman Chemical) by the standard protocol. On the basis of the manufacturer's instructions, the COX-2 Inhibition Screening Assay directly measures $PGF_{2\alpha}$ by $SnCl_2$ reduction of COX-derived PGH_2 produced in the COX reaction. Briefly, a series of supplied reaction buffer solutions with either COX-2 (10 μL) enzyme in the presence of heme (10 μL) were plated in 96-well TC treated plates. Celecoxib **8c**, DIBAC **5**, **4b**&**5** were serially diluted in pre-warmed culture medium immediately before the experiment and added to the wells. The pro-drug **4c** was either added alone or in combination with **5**. Final concentrations of test samples were 25.0, 6.25, 1.56, 0.39, 0.097, 0.024, 0.0060, and 0.0015 μM in 200μL buffer. These solutions were incubated for 3h at 37 °C. Add 10 μL of arachidonic acid (AA, 100μM) and the COX reaction was stopped by the addition of 50 μL of stop solution (stannous chloride) after 2 min at 37 °C. Enzyme immunoassay (EI) measured the reduction product $PGF_{2\alpha}$ from PGH_2 by stannous chloride. This assay is based on the competition between PGs and a PG-acetylcholinesterase conjugate (PG tracer) for a limited amount of PG antiserum. The amount of PG tracer that is able to bind to the PG antiserum is inversely proportional to the concentration of PGs in the wells since the concentration of PG tracer is held constant while the concentration of PGs varies. The plate is washed to remove any unbound reagents and then Ellman's reagent, which contains the substrate to acetylcholine esterase, is added to the well. The product of this enzymatic reaction produces a distinct yellow color that absorbs at 412 nm. The intensity of this color, determined spectrophotometrically, is proportional to the amount of PG tracer bound to the well, which is inversely proportional to the amount of PGs present in the well during the incubation: Absorbance α [Bound PG Tracer] α1/PGs. Percent inhibition was calculated by the comparison of compound-treated to various control incubations. The concentration of the test compound causing 50% inhibition (IC_{50}, μM) was calculated from the concentration-inhibition response curve (**Figure S7**).

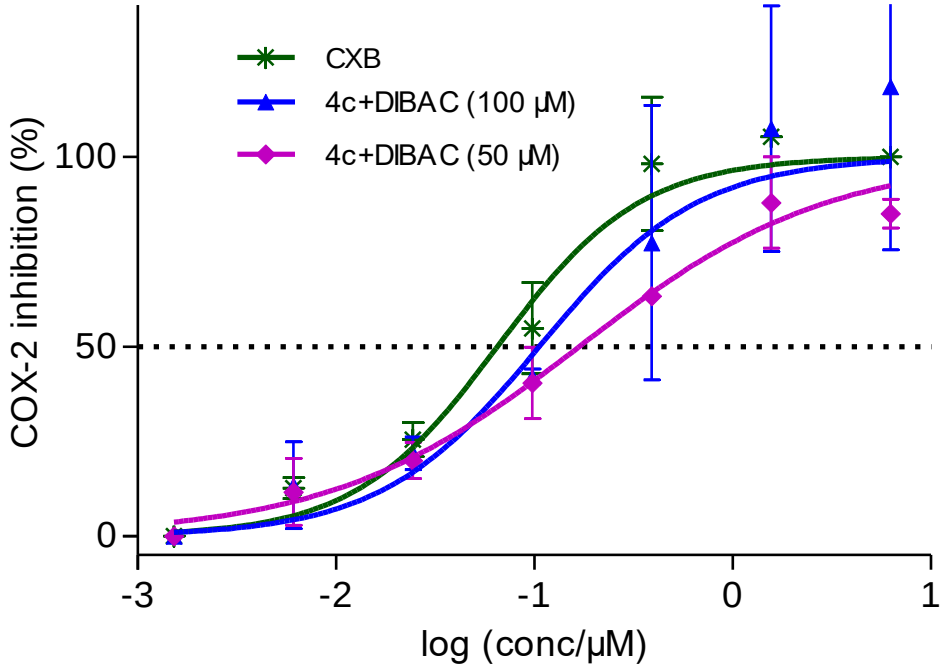

Figure S7. Inhibitions of COX-2 (n=2, error bars represent standard deviation).

Section 8: Mutually orthogonal liberation of two drugs

DIBAC-COOH **5** (0.61 mg, 2×10^{-6} mol) and DPTZ **12** (0.47 mg, 2×10^{-6} mol) were dissolved in 500 μL DMSO-d_6/D_2O (9:1, v/v). The mixture was thoroughly mixed, incubated at room temperature and monitored by ^{1}H NMR spectroscopyat several time points. After 25 h, the components signals stayed the same (**Figure S8**).

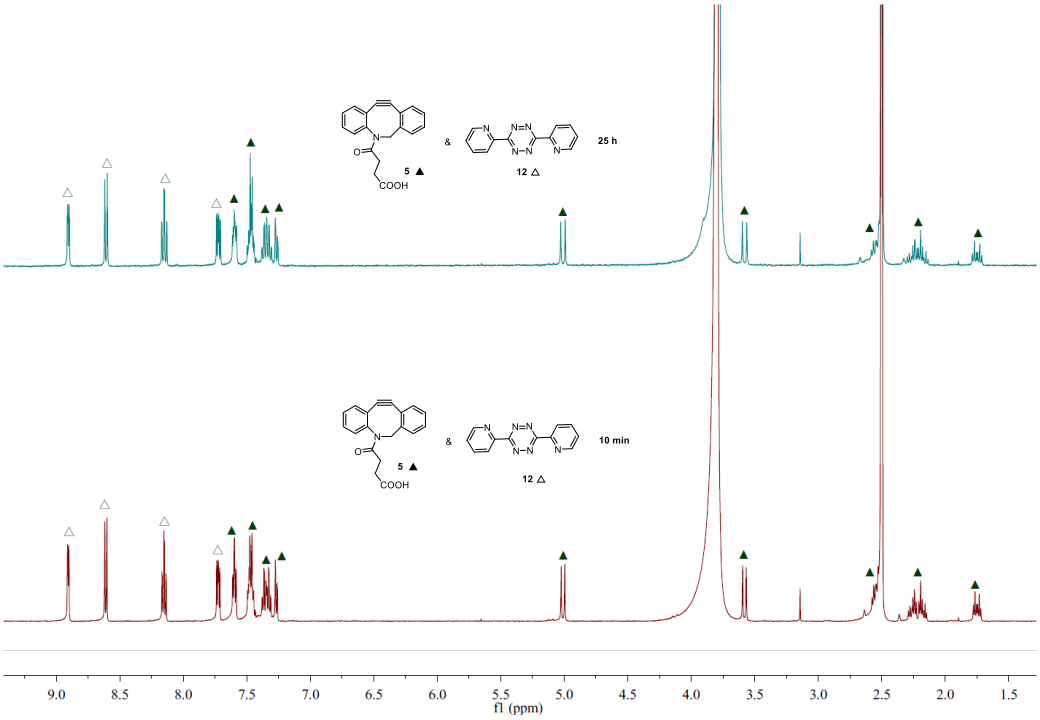

Figure S8. ^{1}H NMR analysis of DIBAC-COOH **5** and DPTz **12** in DMSO-d_6/D_2O (9:1, v/v). Legend: ▲: **5**; △:**12**.

ABNBD-Dox **11** (0.78 mg, 1×10^{-6} mol) and N_6-CXB-SIN **4c** (0.53 mg, 1×10^{-6} mol) were dissolved in 600 μL DMSO-d_6/D_2O (9:1, v/v). The mixture was thoroughly mixed, incubated at room temperature and monitored by ^{1}H NMR spectroscopy at several time points. After 25 h, the components signals did not change (**Figure S9**).

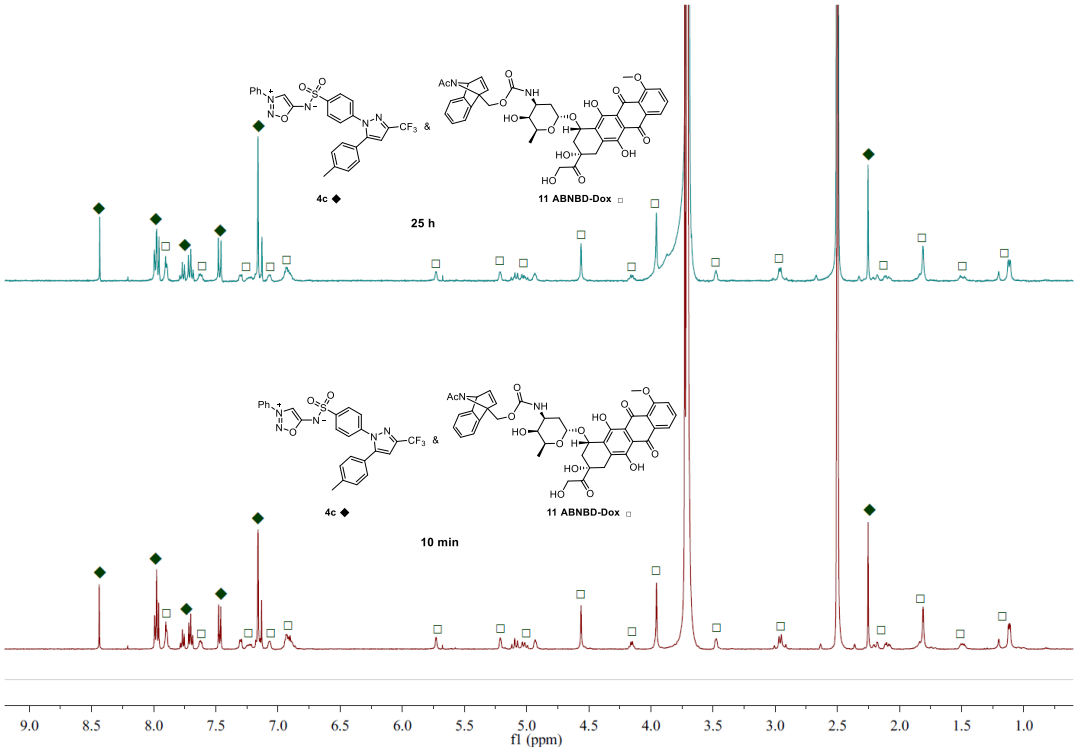

FigureS9. ^{1}H NMR analysis of N_6-CXB-SIN **4c** and ABNBD-Dox **11** in DMSO-d_6/D_2O (9:1, v/v). Legend: ◆: **4c**; □: **11**.

Stock solutions of N_6-CXB-SIN **4c** (15.6 mM), ABNBD-Dox **11** (6.85 mM), DIBAC-COOH **5** (20.5 mM) and DPTz **12** (23.2 mM) in DMSO-d_6 were prepared. Aliquots of **4c** stock solution (64 μL), **11** (146 μL) were combined to give triplicate. Added DIBAC-COOH **5** (245 μL) or DPTz **12** (215μL) or DIBAC-COOH **5** (245 μL) & DPTz **12** (215 μL) to the samples, and added DMSO-d_6/D_2O until final solutions contained DMSO-d_6/D_2O = 9:1, v/v. The progress of the reactions was monitored by ^{1}H NMR spectroscopy at several time points.

As shown in **Figure S10**, after adding DIBAC-COOH **5** to the mixture of N_6-CXB-SIN **4c** and ABNBD-Dox **11**, new signals of cycloaddition product **6** (δ 8.63, 8.62) and released CXB **8c** (δ 7.88) appeared at 10 min, and become much stronger with time. The peaks of **4c** at δ 8.43, δ 8.00, and δ 7.70-7.82 decreased until disappeared to 4.5 h. However, the doxorubicin-prodrug peaks have no change.

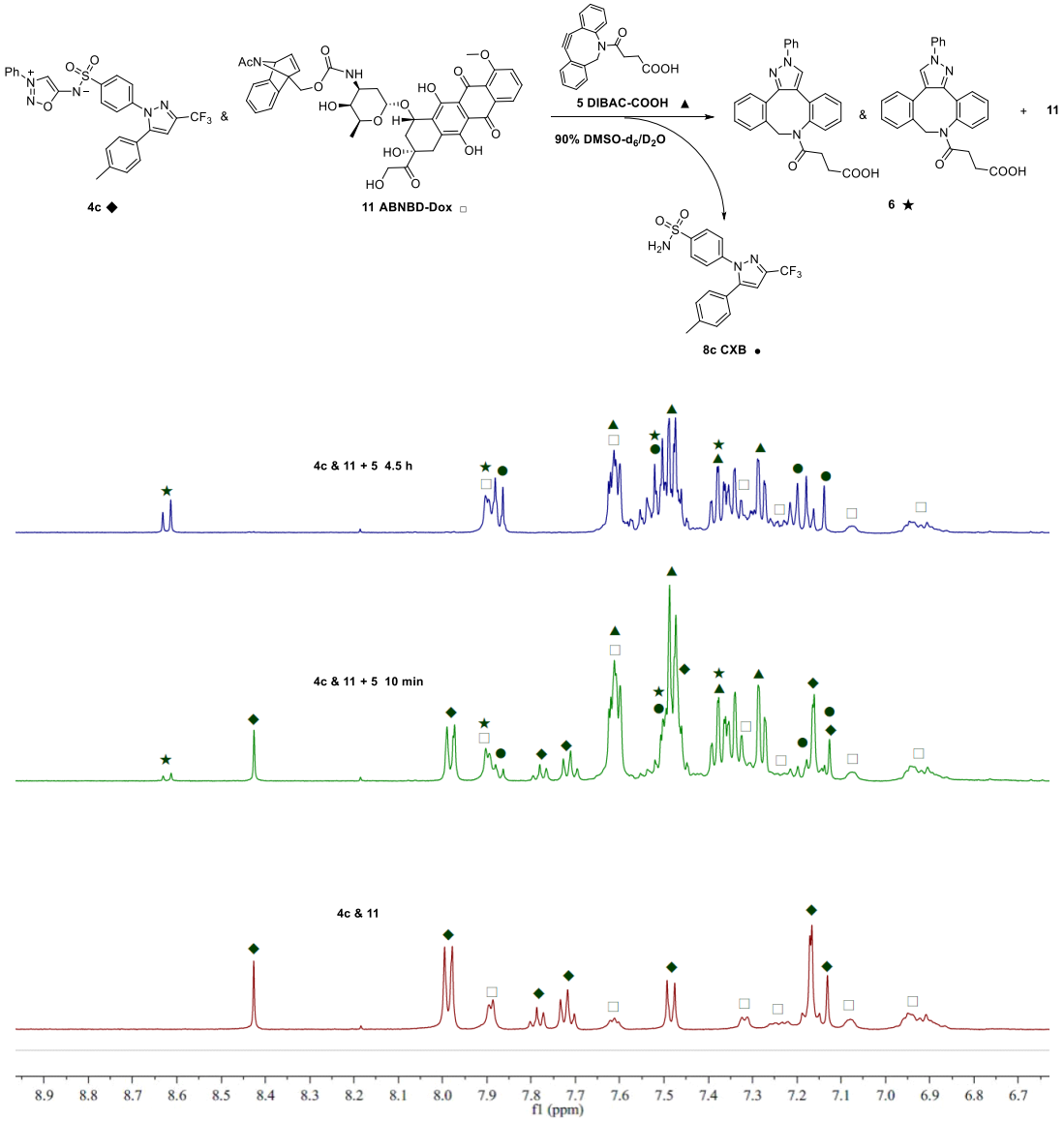

Figure S10. ^{1}H NMR analysis of N_6-CXB-SIN **4c** (1.67 mM) & ABNBD-Dox **11** (1.67 mM) + DIBAC-COOH **5** (8.33 mM) in DMSO-d_6/D_2O (9:1, v/v). Legend: ◆: **4c**; □: **11**; ▲: **5**; ★: **6**;●: **8c**.

As shown in **Figure S11**, to the mixture of N_6-CXB-SIN **4c** and ABNBD-Dox **11** added DPTz **12** DMSO-d_6 solution. As time increases, the peaks of **11** (δ 7.35-7.20, 7.10-7.04, and 6.95-6.85) gradually decayed, and disappeared at the time of 11 h. The new multiplet signals appeared (δ 7.60-7.55) and peak shape (δ 7.91-7.86) changed due to the release of doxorubicin **13**. However, the signals of N_6-CXB-SIN **4c** did not change.

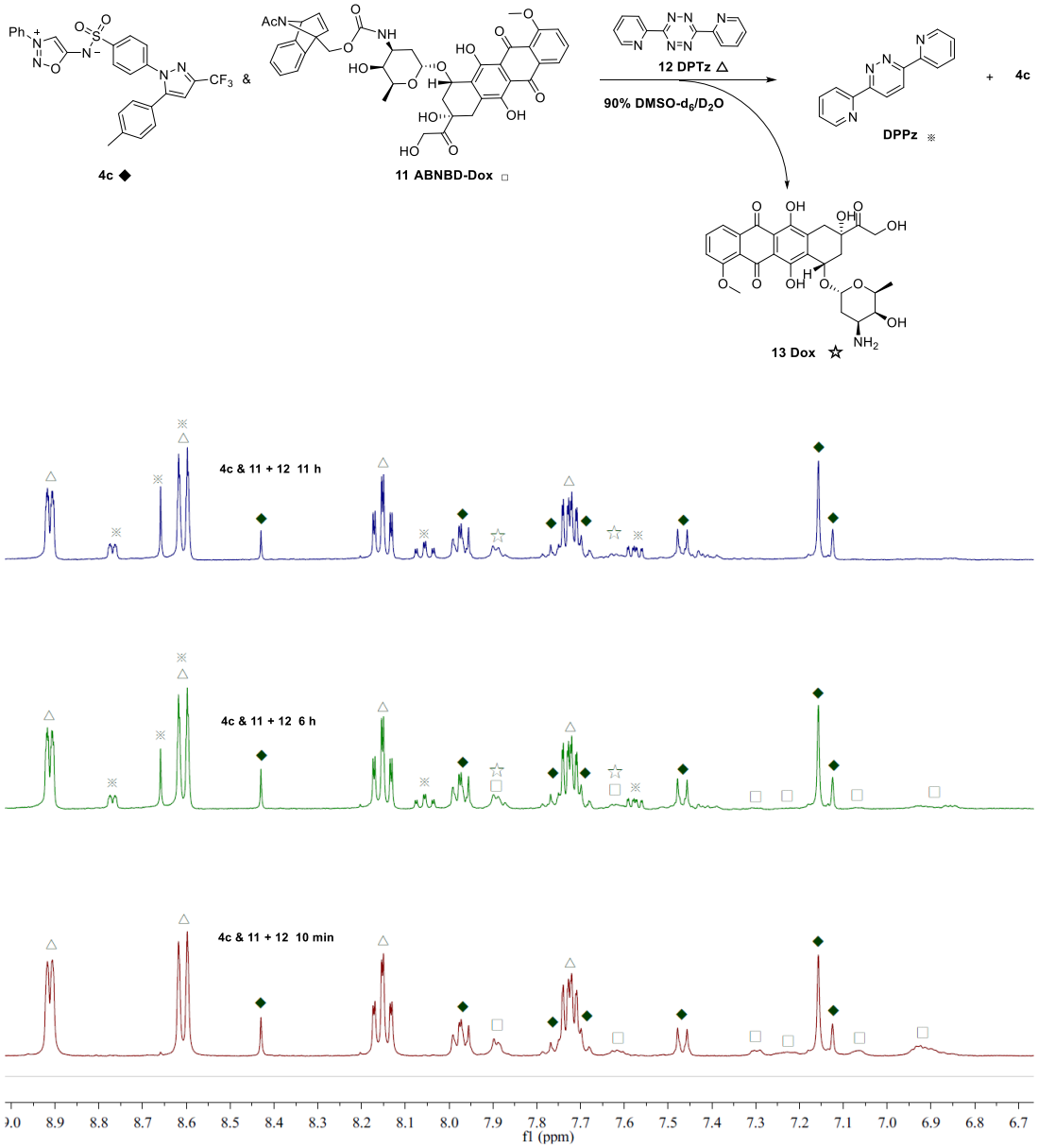

Figure S11. ^{1}H NMR analysis of N_6-CXB-SIN **4c** (1.67 mM) & ABNBD-Dox **11** (1.67 mM) + DPTz **12** (8.33 mM) in DMSO-d_6/D_2O (9:1, v/v). Legend: ◆: **4c**; □: **11**; △: DPTz**12**; ☆: **13**; ※: DPPz.

As shown in **Figure S12**, the mixture of DPTz **12** and DIBAC-COOH **5** was added to the soulation of N_6-CXB-SIN **4c** and ABNBD-Dox **11** in DMSO-d_6/D_2O. The signals of CXB **8c** (δ 7.88) appeared before doxorubicin **14** (δ 7.90). Both peaks of **4c** (δ 8.43 and 8.00-7.95) and **11** (δ 7.10-7.04 and δ 6.95-6.85) were vanished till to 11 h, releasing drug molecules **8c** and **13** completely.

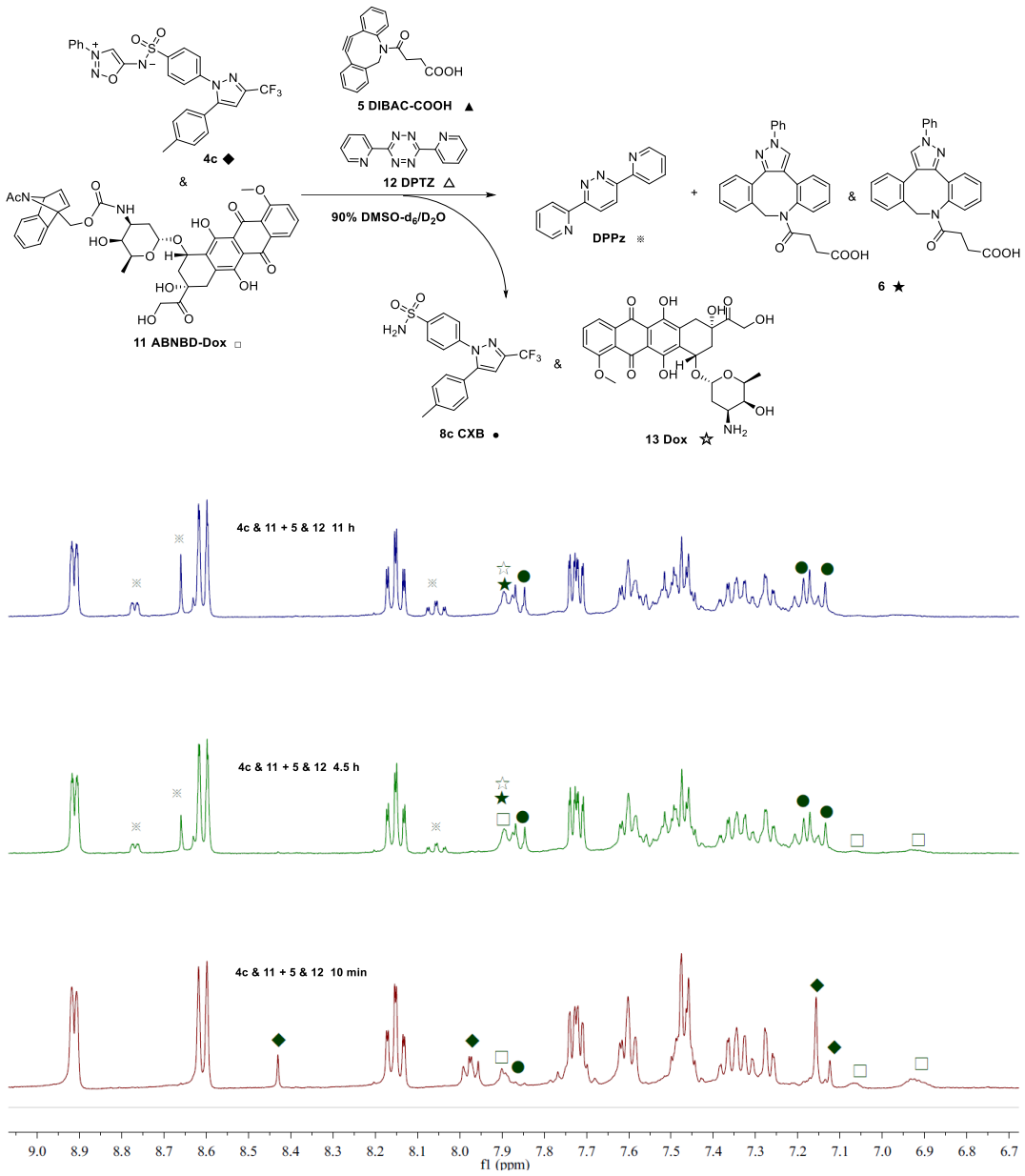

Figure S12. ^{1}H NMR analysis of N_6-CXB-SIN **4c** (1.34 mM) & ABNBD-Dox **11** (1.34 mM) + DPTz **12** (6.72 mM) & DIBAC-COOH **5** (6.72 mM) in DMSO-d_6/D_2O (9:1, v/v). Legend: ◆: **4c**; □: **11**; ▲: **5**; △: **12**; ★: **6**; ●: **8c**; ☆: **13**; ※: DPPz.

Section 9: NMR spectra

^{1}H NMR spectrum of CXB **8c** (500 MHz, $CDCl_3$)

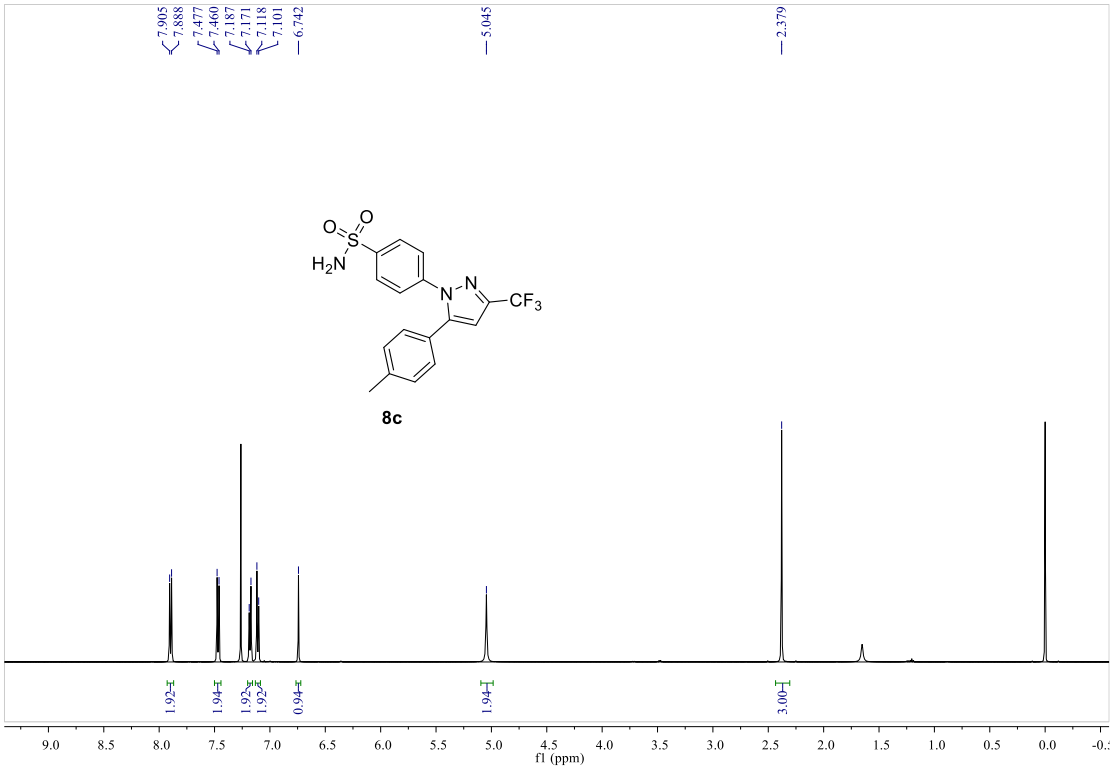

^{13}C NMR spectrum of CXB **8c** (125 MHz, $CDCl_3$)

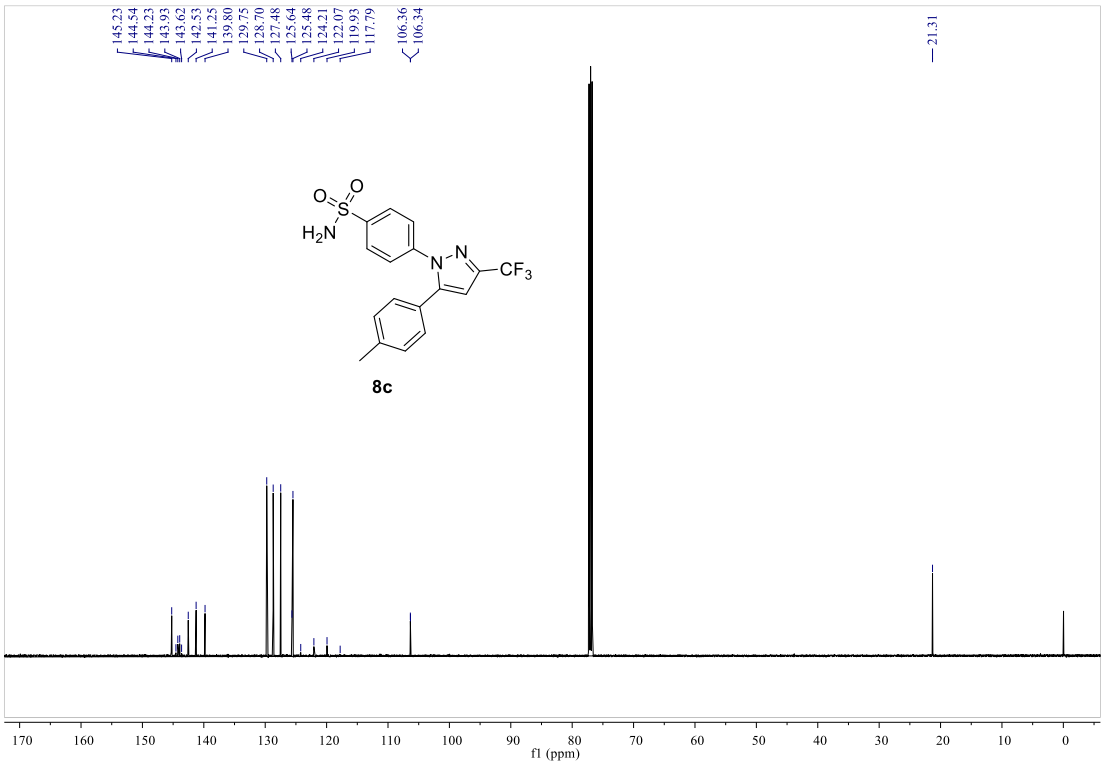

^{19}F NMR spectrum of CXB **8c** (470 MHz, $CDCl_3$)

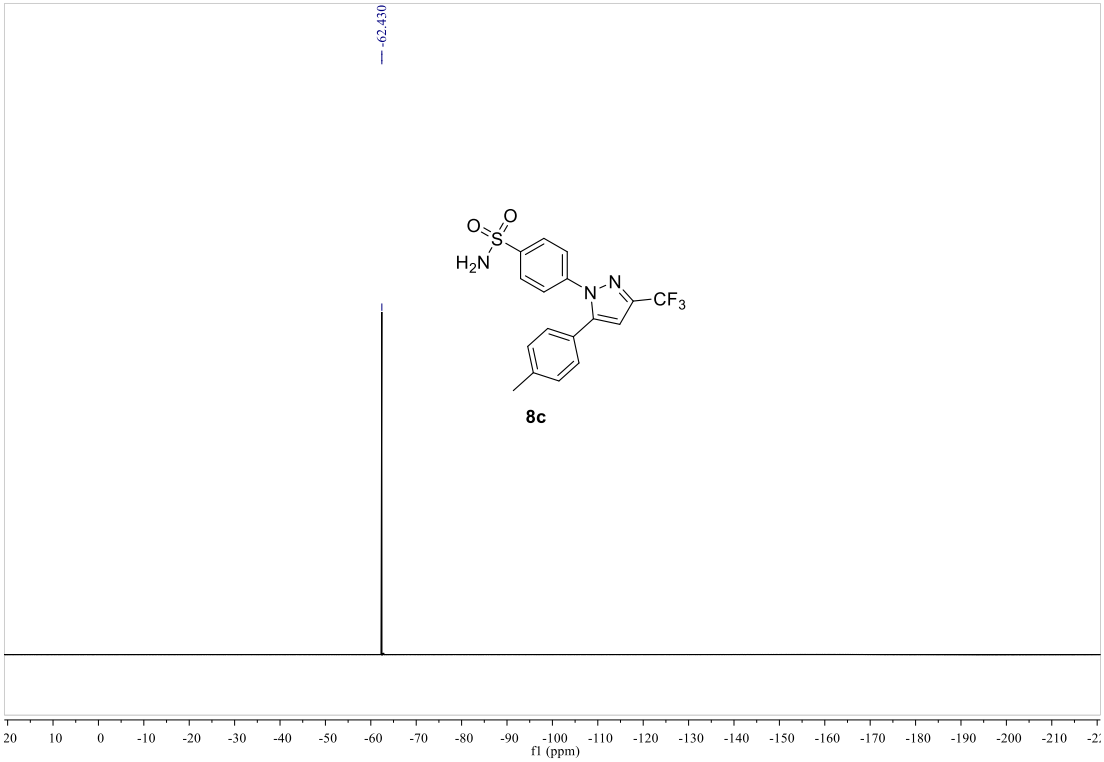

^{1}H NMR spectrum of CXB **8c** (400 MHz, DMSO-d_6)

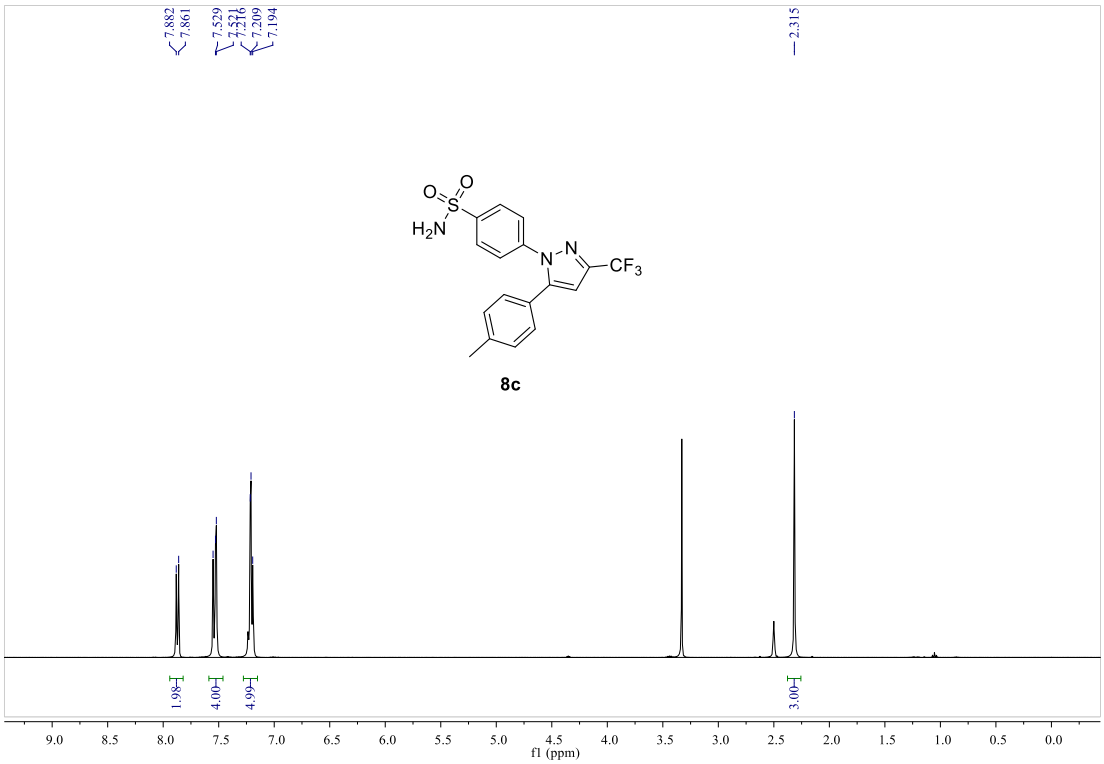

^{1}H NMR spectrum of **9** (400 MHz, DMSO-d_6)

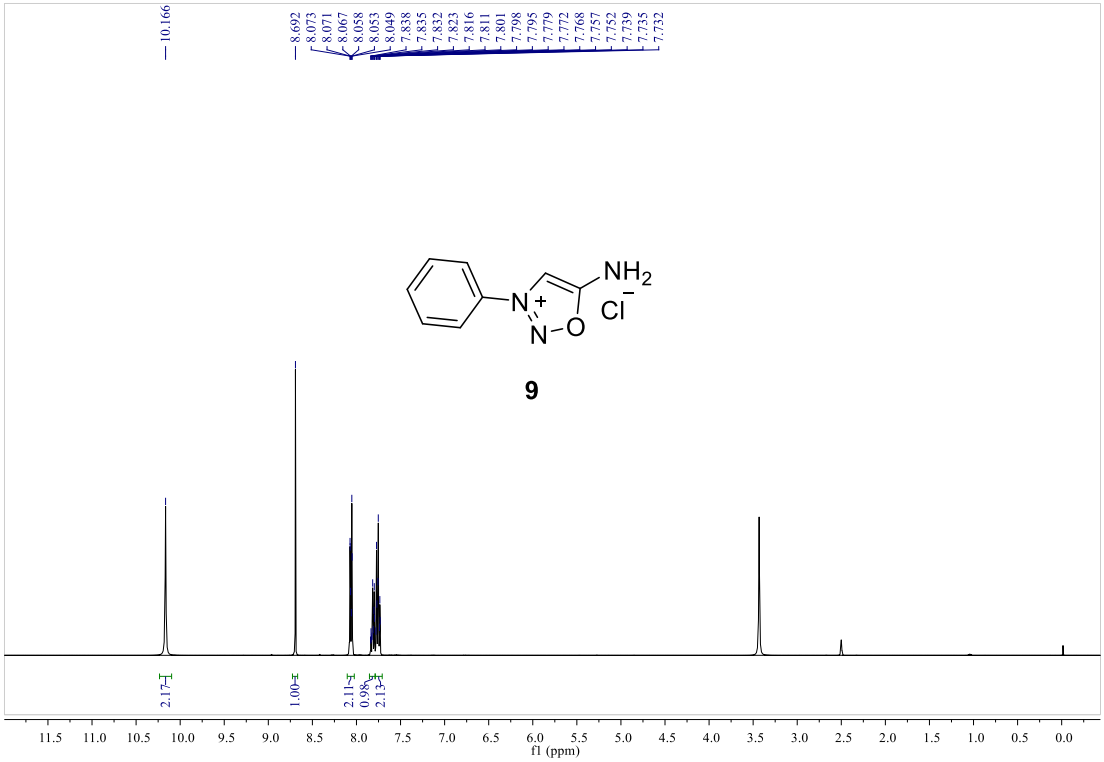

^{13}C NMR spectrum of **9** (100 MHz, DMSO-d_6)

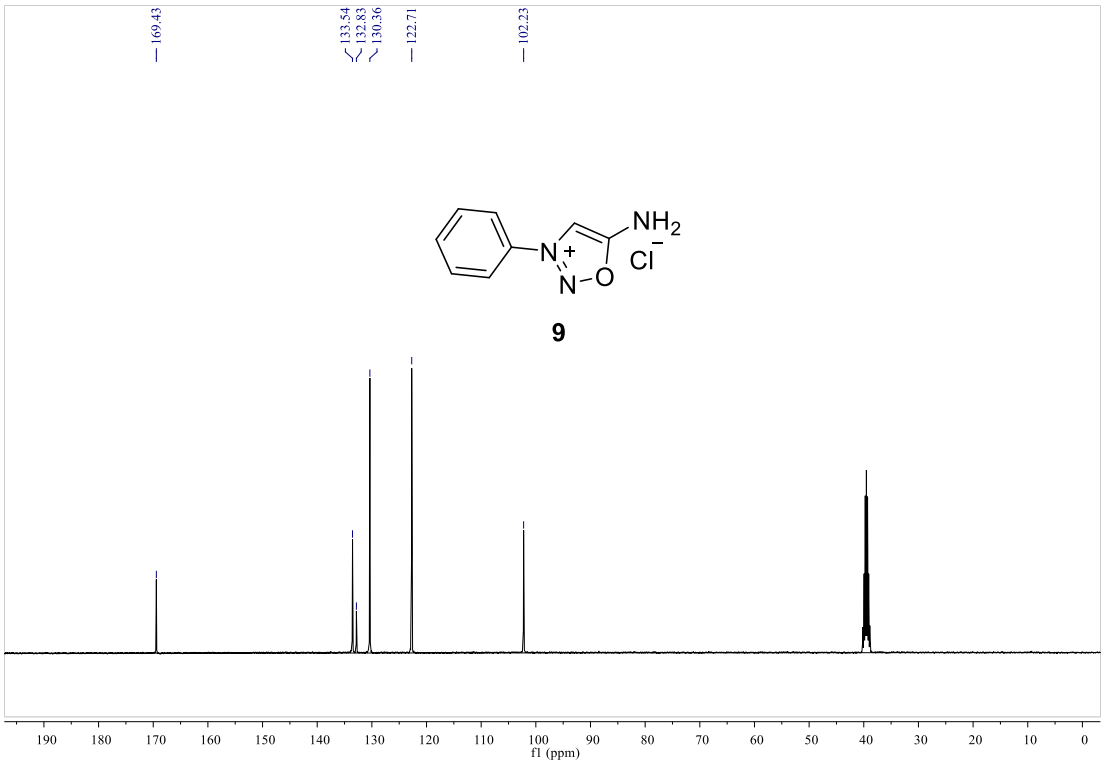

^{1}H NMR spectrum of **9'** (500 MHz, DMSO-d_6)

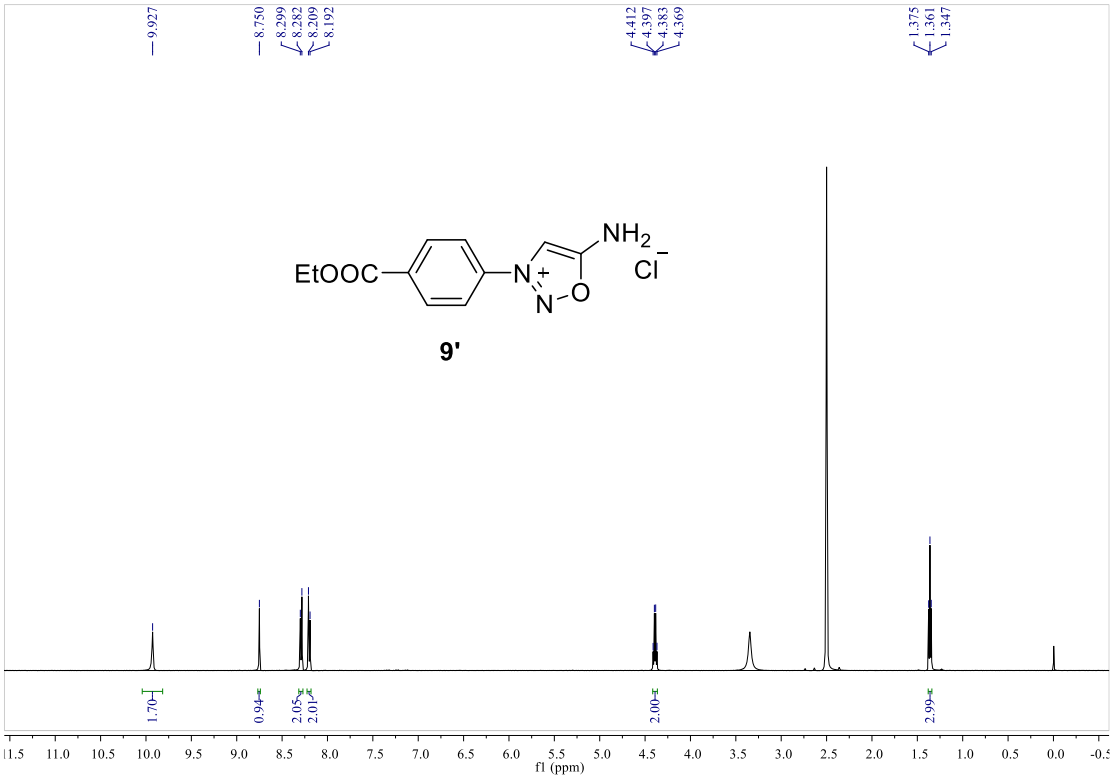

^{13}C NMR spectrum of **9'** (125 MHz, DMSO-d_6)

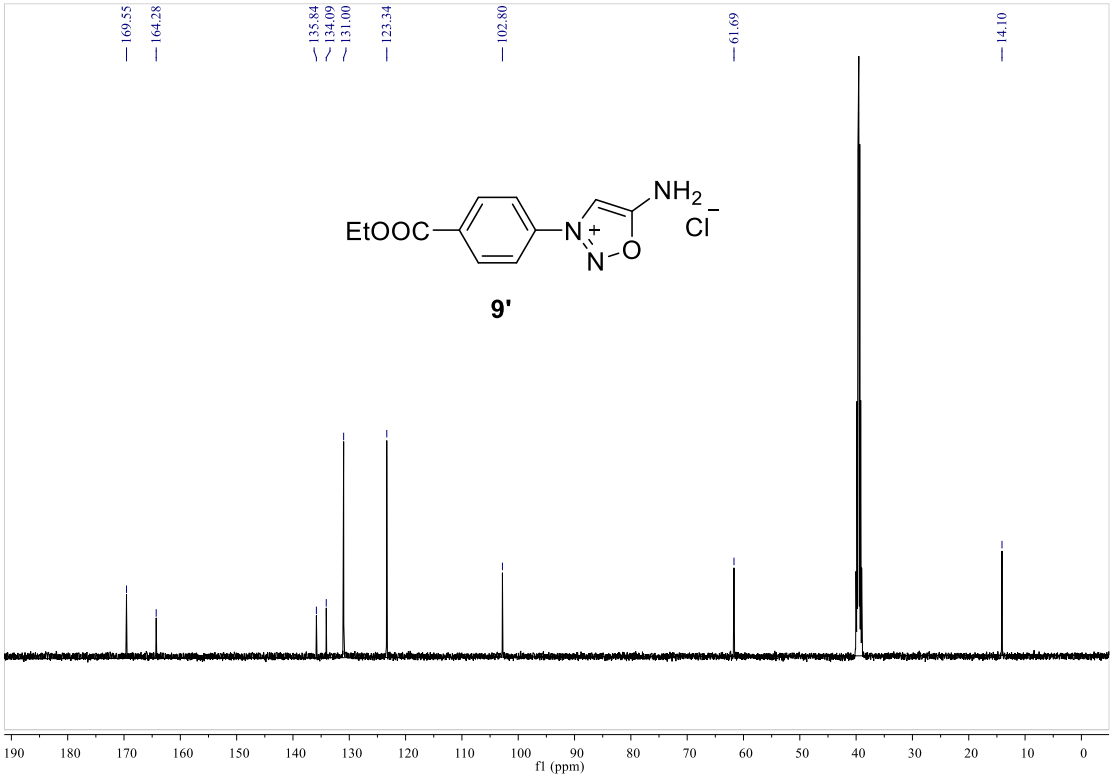

^{1}H NMR spectrum of N_6-Ms-SIN **4a** (400 MHz, DMSO-d_6)

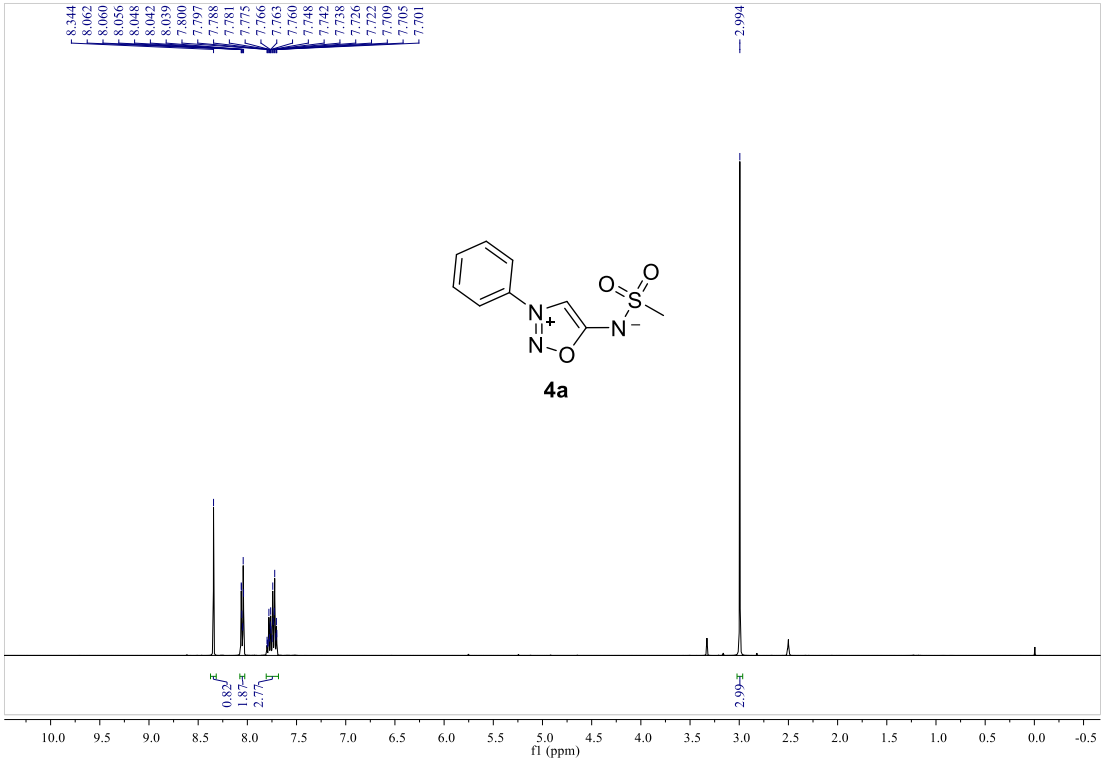

^{13}C NMR spectrum of N_6-Ms-SIN **4a** (100 MHz, DMSO-d_6)

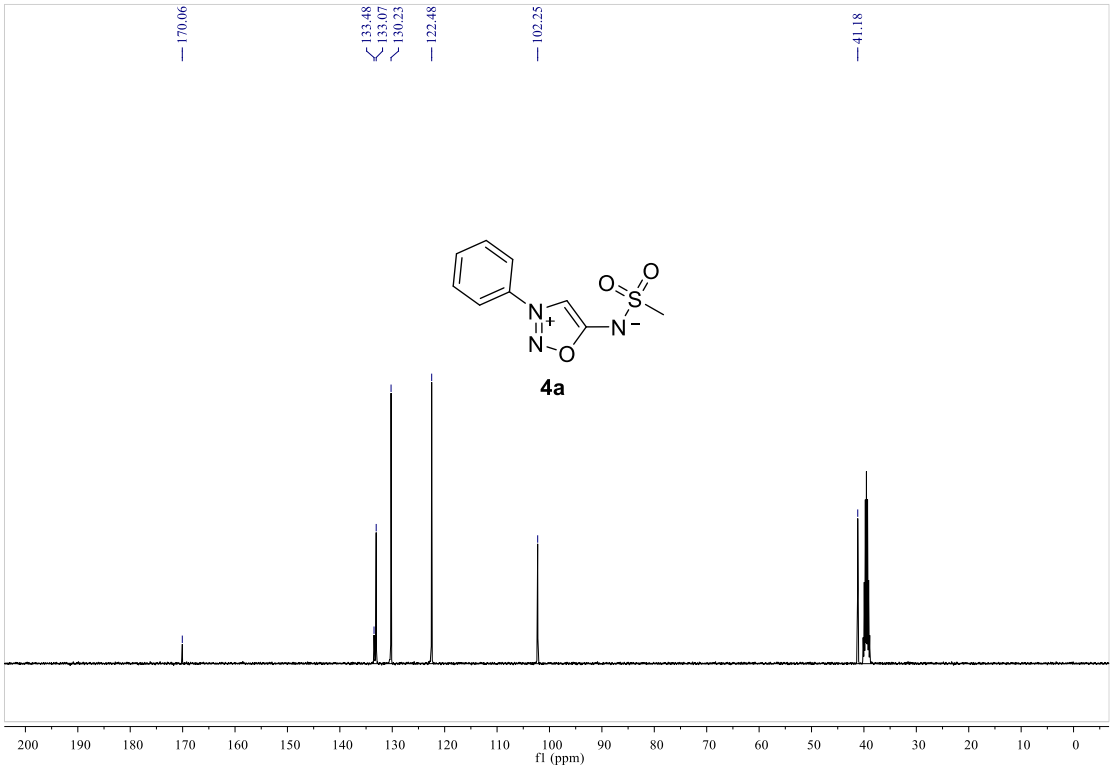

^{1}H NMR spectrum of **4a'** (500 MHz, $CDCl_3$)

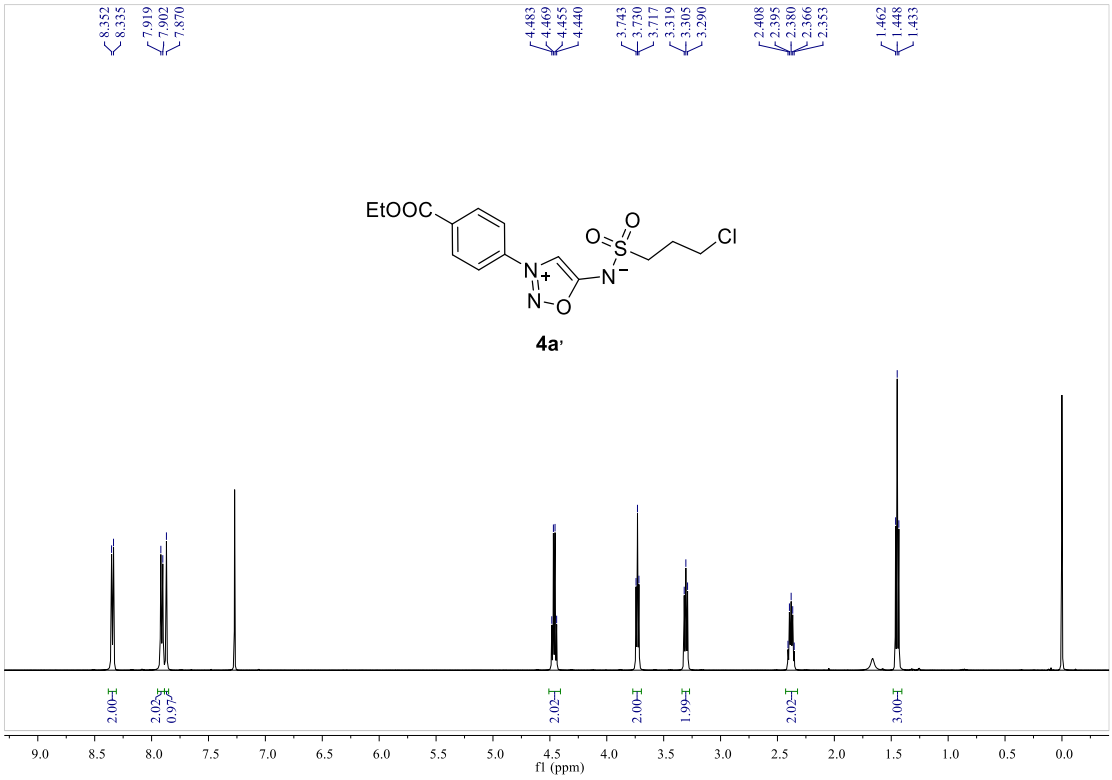

^{13}C NMR spectrum of **4a'** (125 MHz, $CDCl_3$)

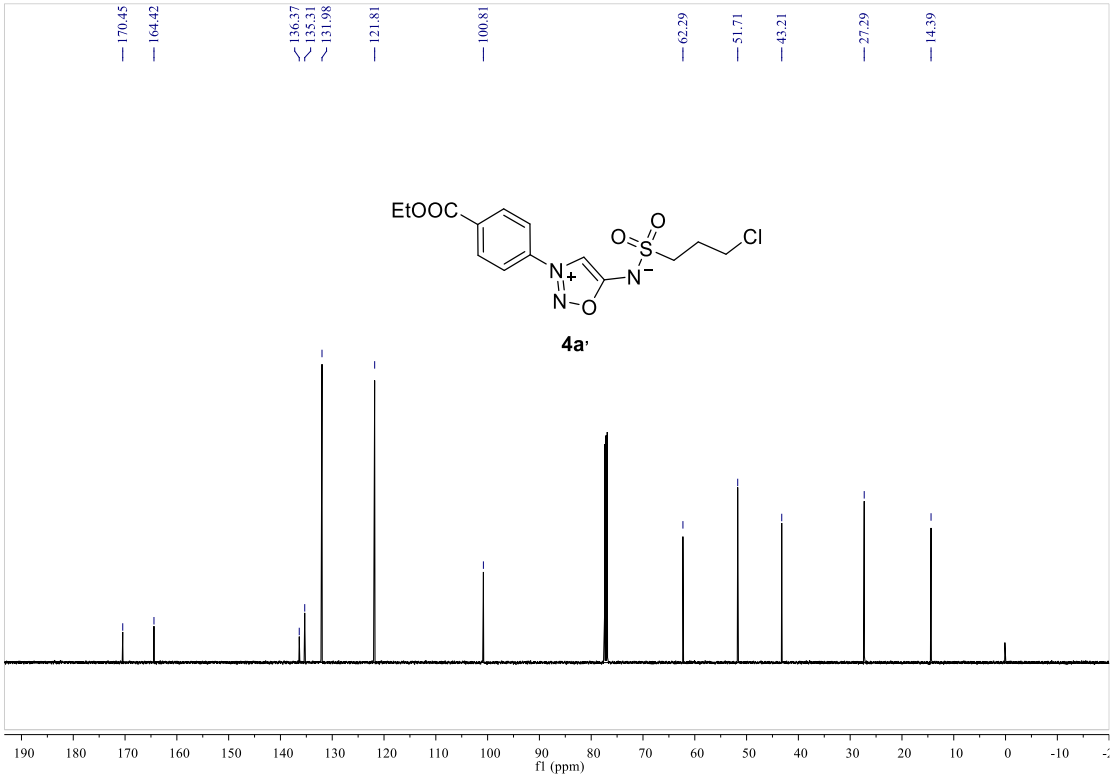

^{1}H NMR spectrum of N_6-Ts-SIN **4b** (400 MHz, DMSO-d_6)

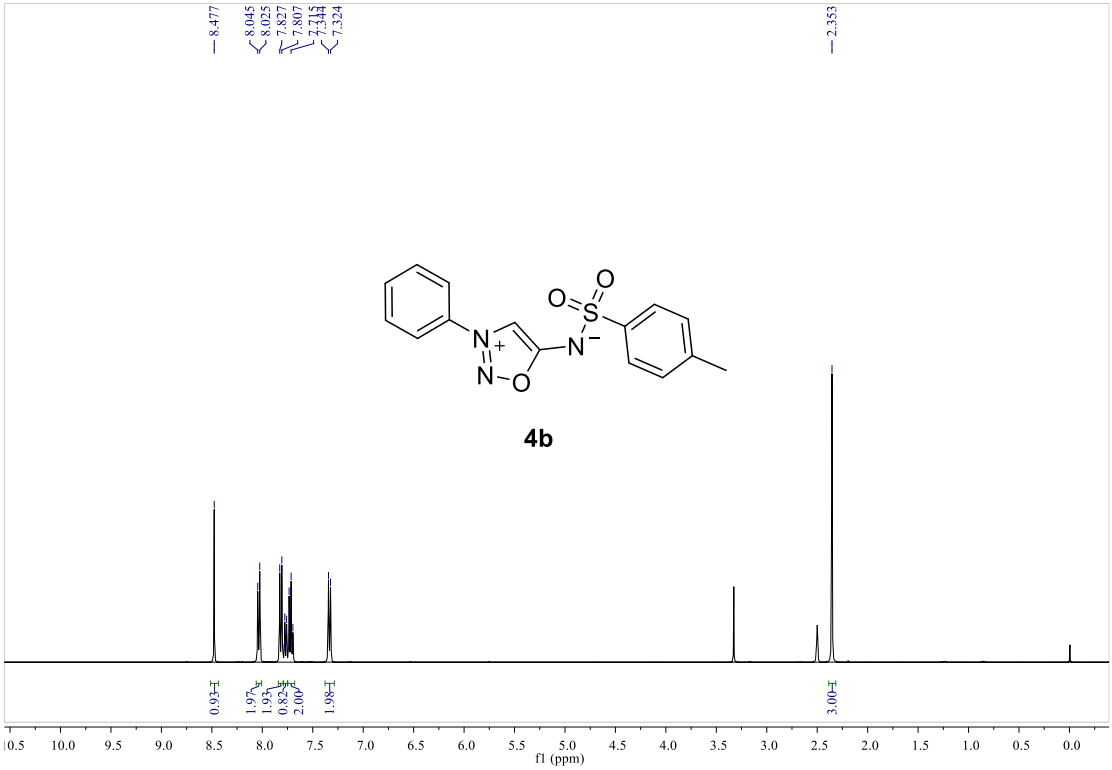

^{13}C NMR spectrum of N_6-Ts-SIN **4b** (100 MHz, DMSO-d_6)

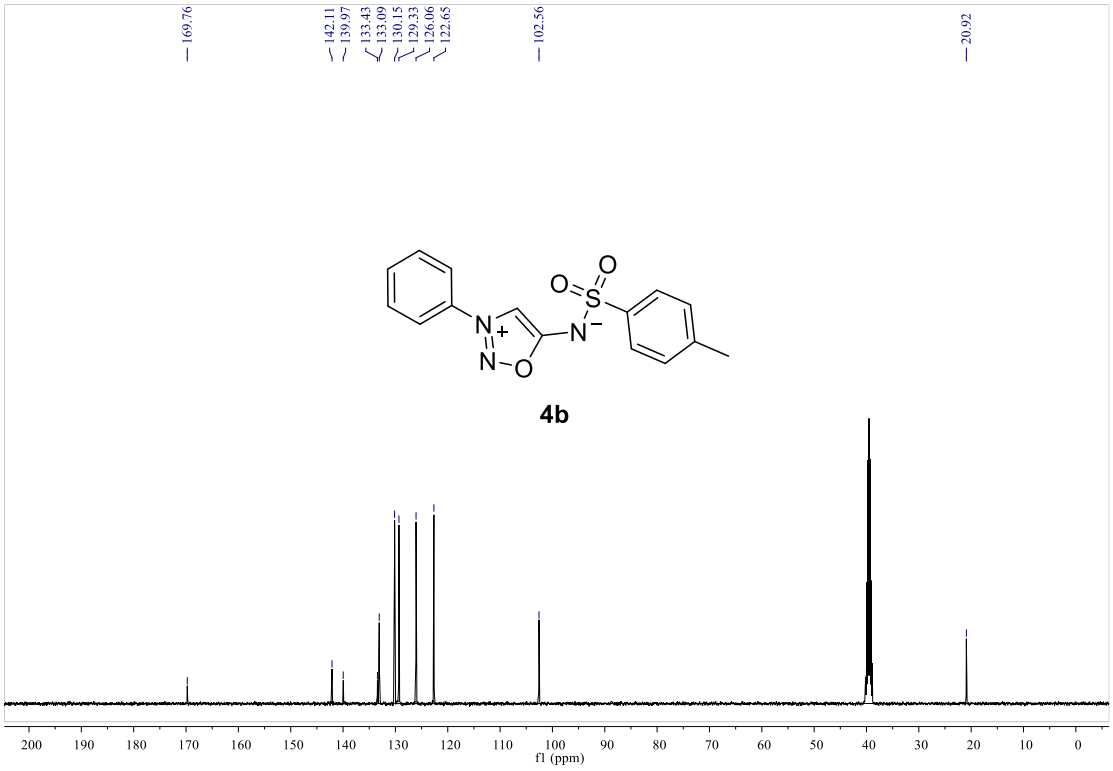

^{1}H NMR spectrum of N_6-CXB-SIN **4c** (600 MHz, DMSO-d_6)

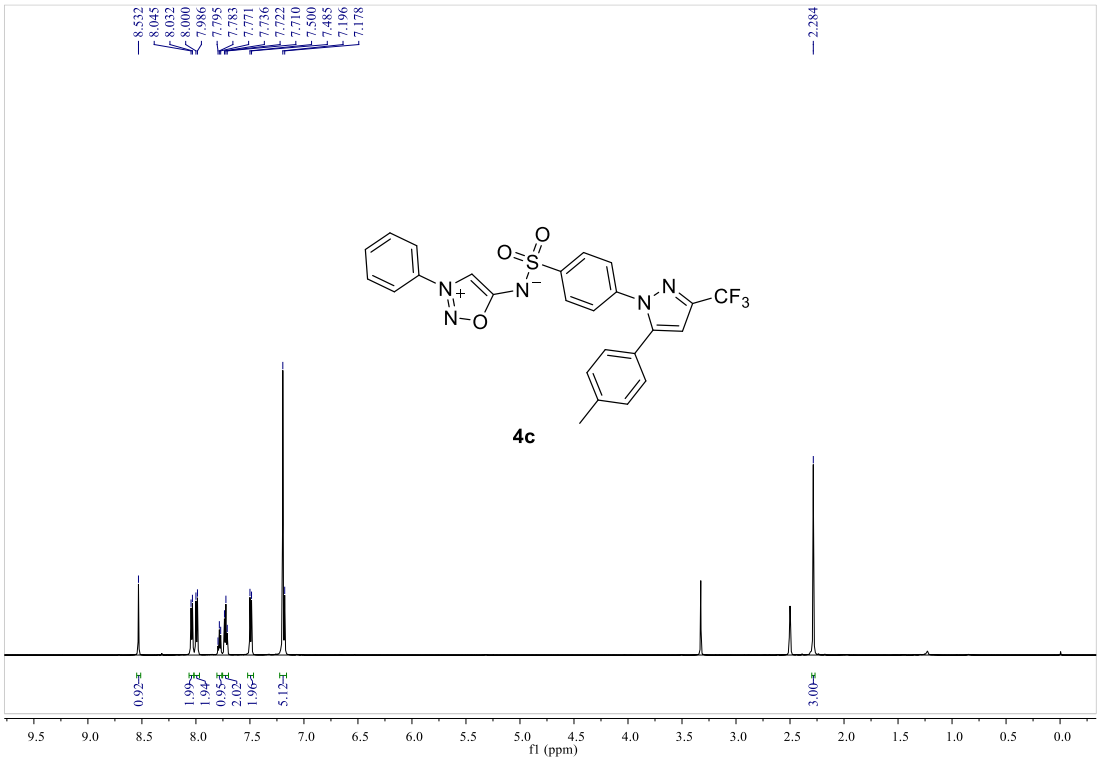

^{13}C NMR spectrum of N_6-CXB-SIN **4c** (150 MHz, DMSO-d_6)

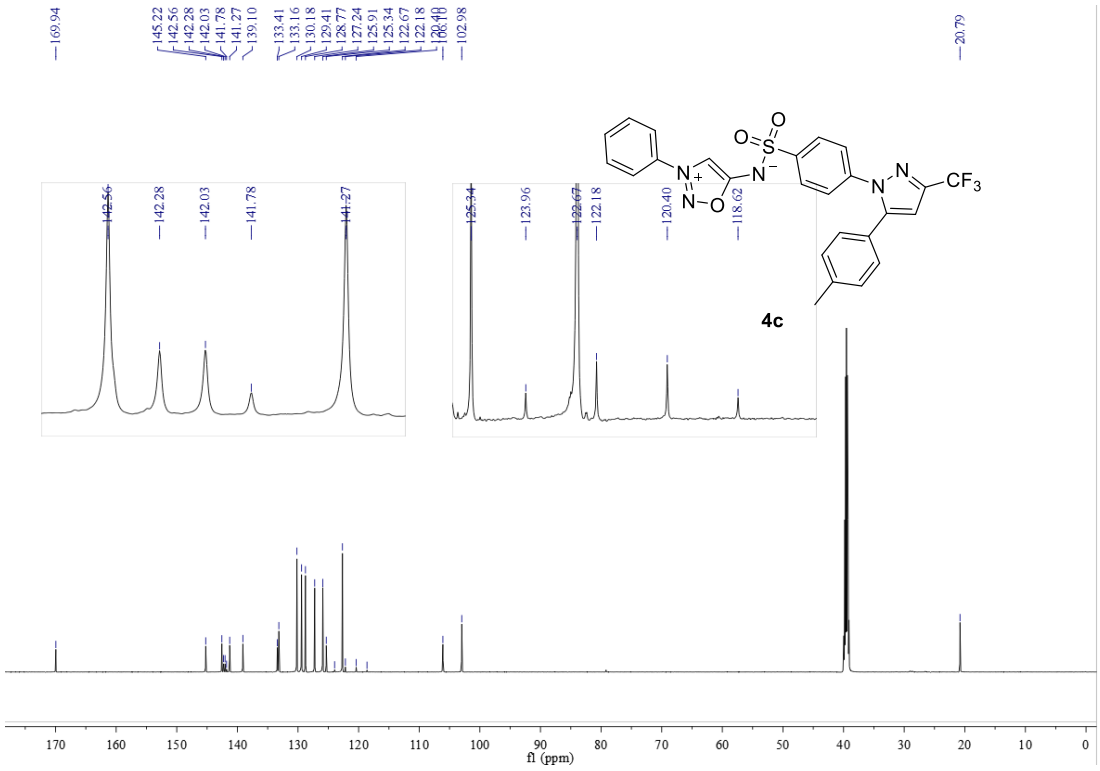

^{19}F NMR spectrum of N_6-CXB-SIN **4c** (470 MHz, DMSO-d_6)

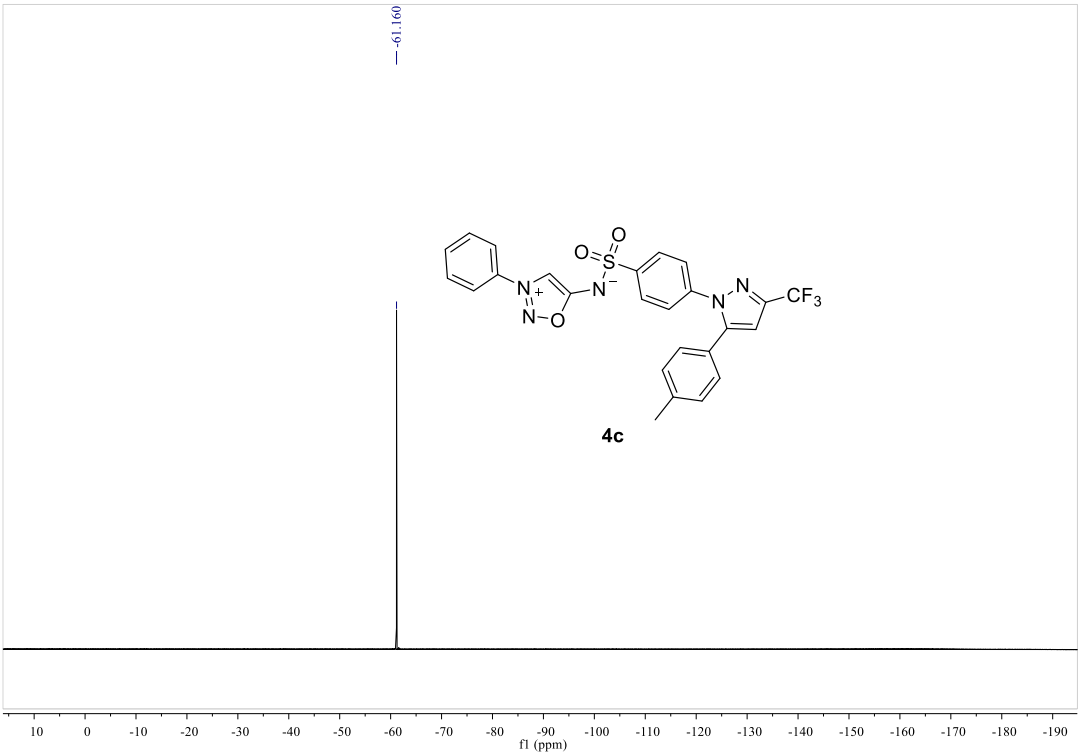

^{1}H NMR spectrum of **6** (600 MHz, DMSO-d_6)

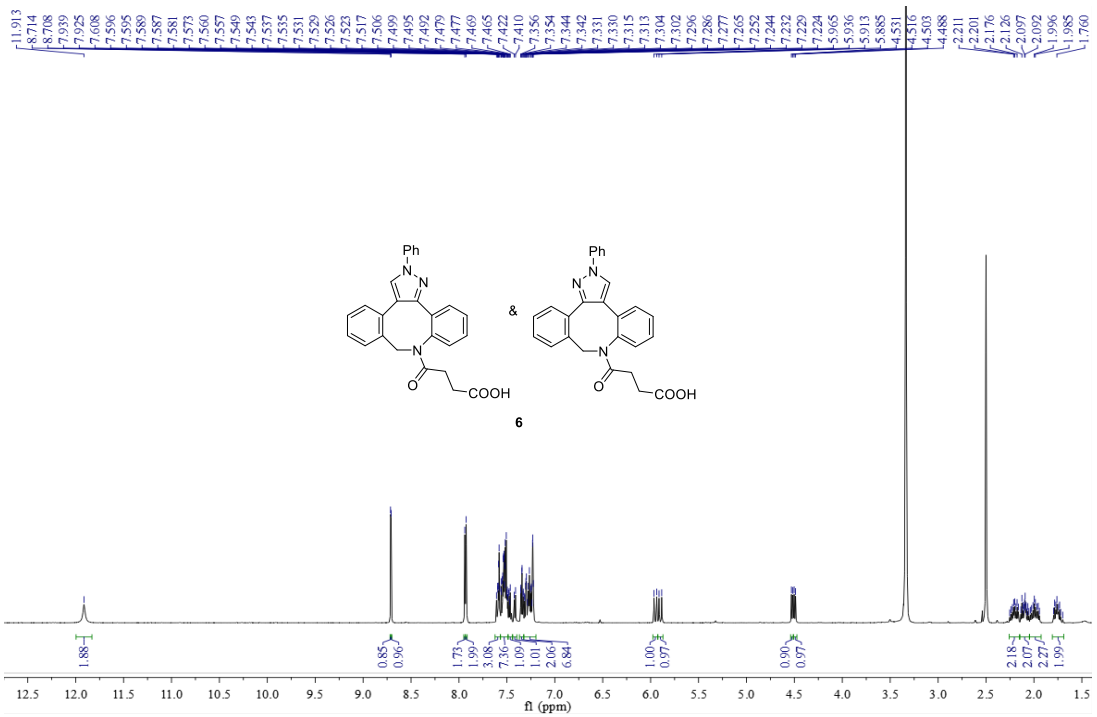

^{13}C NMR spectrum of **6** (150 MHz, DMSO-d_6)